

MICROCOPY RESOLUTION TEST CHART
NATIONAL BUREAU OF STANDARDS 1963-A

LEVEL II

2

AD A098813

NAVAL POSTGRADUATE SCHOOL
Monterey, California

Master's thesis



DTIC
ELECTE
MAY 13 1981
S D
E

12 117

6

THESIS

TEST OF THE APPLICATION OF THE TYWAVES
MODEL TO PREDICTION OF SWELL IN THE EAST
CHINA SEA FROM THREE TROPICAL CYCLONES IN
THE WESTERN NORTH PACIFIC.

by

Lee Hyong Sun / Lee

11 December 1980

Thesis Advisor:

J. B. Wickham

Approved for public release; distribution unlimited

DTIC FILE

251450 Fin

81 5 12 032

UNCLASSIFIED

SECURITY CLASSIFICATION OF THIS PAGE (When Data Entered)

REPORT DOCUMENTATION PAGE		READ INSTRUCTIONS BEFORE COMPLETING FORM
1. REPORT NUMBER	2. GOVT ACCESSION NO.	3. RECIPIENT'S CATALOG NUMBER
	AD-A098813	
4. TITLE (and Subtitle) Test of the Application of the TYWAVES Model to Prediction of Swell in the East China Sea from Three Tropical Cyclones in the Western North Pacific		5. TYPE OF REPORT & PERIOD COVERED Master's Thesis; December 1980
7. AUTHOR(s) Lee, Hyong Sun		6. PERFORMING ORG. REPORT NUMBER
9. PERFORMING ORGANIZATION NAME AND ADDRESS Naval Postgraduate School Monterey, California 93940		8. CONTRACT OR GRANT NUMBER(s)
11. CONTROLLING OFFICE NAME AND ADDRESS Naval Postgraduate School Monterey, California 93940		10. PROGRAM ELEMENT, PROJECT, TASK AREA & WORK UNIT NUMBERS
13. MONITORING AGENCY NAME & ADDRESS (if different from Controlling Office) Naval Postgraduate School Monterey, California 93940		12. REPORT DATE December 1980
		13. NUMBER OF PAGES 116 pages
		14. SECURITY CLASS. (of this report) Unclassified
		15. DECLASSIFICATION/DOWNGRADING SCHEDULE
16. DISTRIBUTION STATEMENT (of this Report) Approved for public release; distribution unlimited		
17. DISTRIBUTION STATEMENT (of the abstract entered in Block 20, if different from Report)		
18. SUPPLEMENTARY NOTES		
19. KEY WORDS (Continue on reverse side if necessary and identify by block number) TYWAVES, typhoons, wave propagation.		
20. ABSTRACT (Continue on reverse side if necessary and identify by block number) A method for predicting swell from tropical cyclones using a spectral wave model (TYWAVES) was tested. The model was applied to predicting swell propagating from three typhoons in the Western North Pacific through gaps in the Ryukyu Islands into a region of the East China Sea. The model involves a source region concept which considers only the swell emanating from regions of peak energy in moving typhoons. For three representative typhoons predicted heights were not significantly different from the		

Correct page

UNCLASSIFIED

SECURITY CLASSIFICATION OF THIS PAGE/When Data Entered

observed heights. The time of occurrence of the predicted peak height agreed well with observational values for the swell from two typhoons, but lagged by 6-12 hours for the third.

The dominant swell period and direction predicted by the model were not verifiable by data available for this study.

Shoaling and refraction effects were considered in the prediction, in a simplified way, but attenuation was ignored even for the passage of energy through the Ryukyu Islands.

Accession For	
NTIS GRA&I	<input checked="" type="checkbox"/>
DTIC TAB	<input type="checkbox"/>
Unannounced	<input type="checkbox"/>
Justification	
By	
Distribution/	
Availability Codes	
Dist	Special
A	

Approved for public release; distribution unlimited

Test of the Application of the TYWAVES
Model to Prediction of Swell in the East
China Sea from Three Tropical Cyclones in
the Western North Pacific

by

Hyong Sun Lee
Lieutenant Commander, Republic of Korea Navy
B.S., Republic of Korea Naval Academy, 1972

Submitted in partial fulfillment of the
requirements for the degree of

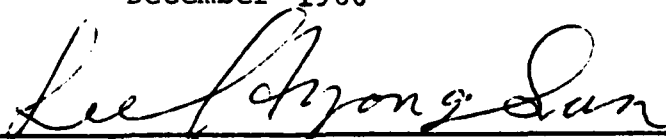
MASTER OF SCIENCE IN OCEANOGRAPHY

from the

NAVAL POSTGRADUATE SCHOOL

December 1980

Author



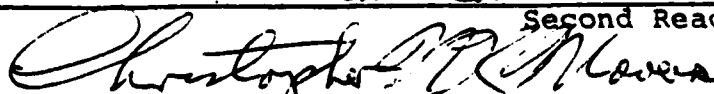
Approved by:



Thesis Advisor



Second Reader



Chairman, Department of Oceanography



Dean of Science and Engineering

ABSTRACT

A method for predicting swell from tropical cyclones using a spectral wave model (TYWAVES) was tested. The model was applied to predicting swell propagating from three typhoons in the Western North Pacific through gaps in the Ryukyu Islands into a region of the East China Sea. The model involves a source region concept which considers only the swell emanating from regions of peak energy in moving typhoons. For three representative typhoons, predicted heights were not significantly different from the observed heights. The time of occurrence of the predicted peak height agreed well with observational values for the swell from two typhoons, but lagged by 6-12 hours for the third.

The dominant swell period and direction predicted by the model were not verifiable by data available for this study.

Shoaling and refraction effects were considered in the prediction, in a simplified way, but attenuation was ignored even for the passage of energy through the Ryukyu Islands.

TABLE OF CONTENTS

I. INTRODUCTION----- 11

 A. OBJECTIVE OF THE STUDY----- 11

 B. TYPHOONS IN THE WESTERN NORTH PACIFIC----- 11

 C. TYWAVES MODEL (THE TYPHOON WAVES PROGRAM)---- 12

 D. FORECASTING AND VERIFICATION----- 13

 E. TERMINOLOGY----- 22

II. PREDICTION OF TROPICAL STORM WAVES BY TYWAVES
MODEL----- 25

 A. LOCATION OF THE SELECTED POINT-SOURCES----- 25

 B. SEA-SPECTRA AT THE POINT-SOURCES----- 28

 C. SELECTION OF THE DIRECTIONAL ENERGY AT
 POINT-SOURCES----- 29

 D. TOTAL AND DIRECTIONAL ENERGY AT POINT-
 SOURCES----- 30

 1. Typhoon Hope----- 31

 2. Typhoon Irving----- 31

 3. Typhoon Owen----- 32

III. PREDICTION OF SWELL CHARACTERISTICS----- 36

 A. THE SETTING OF THE FORECAST SITE AND ITS
 RELATION TO THE WAVE SOURCES----- 36

 B. GROUP VELOCITY----- 37

 C. TRAVEL DISTANCE AND ARRIVAL TIME----- 39

IV. THE ENERGY PROPAGATION PROCEDURE----- 45

 A. PROPAGATION OF SPECTRAL ENERGY COMPONENTS---- 45

B.	SHOALING AND REFRACTION FACTOR-----	47
1.	Shoaling Factor-----	47
2.	Refraction Factor-----	50
C.	SHOALING AND REFRACTION OF THE SPECTRAL COMPONENTS-----	51
1.	Shoaling Process (Computations)-----	52
2.	Shoaling Energy Components From Each Source Versus Arrival Time-----	52
3.	The Predicted Swell Waves at Prediction Site-----	53
D.	OBSERVED DATA-----	53
E.	COMPARISON OF SWELL PREDICTIONS AND OBSERVATIONS-----	63
F.	ERROR SOURCES-----	64
V.	CONCLUSIONS-----	67
	APPENDIX A (Outputs of TYWAVES for Typhoon Owen on 12 GMT September 26)-----	68
	APPENDIX B (Sea Spectra at Source Region for Three Typhoons and Significant Wave Distribution)-	76
	APPENDIX C (Propagation Energy Arrival Time)-----	89
	APPENDIX D (Shoaling of the Spectral Energy Components)-	94
	LIST OF REFERENCES-----	113
	INITIAL DISTRIBUTION LIST-----	115

LIST OF TABLES

1.	1979 Significant Tropical Cyclones-----	14
2.	1979 Significant Tropical Cyclone Statistics-----	14
3.	Best Track for Super Typhoon Hope-----	19
4.	Best Track for Typhoon Irving-----	20
5.	Best Track for Typhoon Owen-----	20
6.	Typhoon Centers and Selected Points Location-----	27
7.	Period-Directional Spectrum at Point 4 of 06 GMT September 25, 1979-----	30
8.	The Visual Observation Data by NODC and ROK Navy-	60

LIST OF FIGURES

1. Typhoon Tracks-----	15
2. Typhoon Hope, Best Track-----	16
3. Typhoon Irving, Best Track-----	18
4. Typhoon Owen, Best Track-----	17
5. Possible Refraction Diagram at Point 4 at 06 GMT September 25, 1979-----	29
6. Typhoon Hope, Total and Directional Energies at Point Sources-----	33
7. Typhoon Irving, Total and Directional Energies at Point Sources-----	34
8. Typhoon Owen, Total and Directional Energies at Point Sources-----	35
9. Typhoon Hope Swell Arrival Time-----	42
10. Typhoon Irving Swell Arrival Time-----	43
11. Typhoon Owen Swell Arrival Time-----	44
12. Typhoon Hope, Directional Energy Propagation-----	54
13. Typhoon Hope, Total Propagated Energy Comparison---	57
14. Typhoon Irving, Directional Energy Propagation-----	55
15. Typhoon Irving, Total Propagated Energy Comparison-	58
16. Typhoon Owen, Directional Energy Propagation-----	56
17. Typhoon Owen, Total Propagated Energy Comparison---	59

LIST OF MAP AND PLATE

MAP 1. East China Sea Bottom Contours-----	21
PLATE C-1. Illustration of Various Functions of $\frac{d}{L_0}$ ----	48
FIGURE 2-19. Changes in Wave Direction and Height Due to Refraction on Slopes with Straight Parallel Depth Contours-----	49

ACKNOWLEDGMENTS

I wish to express my deepest thanks to Professor J. B. Wickham for the concepts and methods in this thesis. The completion of this work is due to his effort, experience and guidance.

I also wish to recognize the invaluable cooperation and assistance of Samson Brand, Naval Environmental Prediction Research Facility, Monterey, California, 93940; Kevin M. Rabe, Science Applications International, Monterey, California, 93940; and of Professor J. Von Schwind, Naval Postgraduate School, Monterey, California, 93940.

I. INTRODUCTION

A. OBJECTIVE OF THE STUDY

A serious problem for naval activities, ocean industry, shore protection and fisheries in the Korean south coastal area is the lack of adequate estimation of the waves resulting from typhoons. The objective of this study is to make a partial test of the TYWAVES for forecasting swell from tropical cyclones which arrive at a single observation site near Cheju-do, Korea (33.2°N 126.6°E).

Forecasting based on wave fields predicted in a typhoon area by the TYWAVES [13] developed by NEPRF (Naval Environmental Prediction Research Facility) are to be verified against swell observations made near Cheju-do.

B. TYPHOONS IN THE WESTERN NORTH PACIFIC

During 1979, the Western North Pacific experienced 28 tropical cyclones. Table I, from "1979 Annual Typhoon Report" [2], shows the significant tropical cyclones for that year. Table II from [2] shows the monthly distribution of tropical cyclones in 1979 and other statistics.

Most typhoons occur in the summer season and their tracks can be classified as one of three typical tracks. The first type is that passing south of Taiwan toward the west, the second is that crossing over Korea through the

Ryukyu Islands, and the third is that passing east of Ryukyu Islands.

I selected one typhoon of each type; one each in July, August, and September in 1979. They are Typhoons Hope, Irving and Owen shown in Figures 1, 2, 3 and 4 from [2]. tropical cyclone "best track" information is shown in Tables III, IV, and V for Typhoon Hope, Irving and Owen, respectively.

C. TYWAVES MODEL (THE TYPHOON WAVES PROGRAM)

The SOWM (Spectral Ocean Wave Model) run at FNOC (Fleet Numerical Oceanography Center) utilizes a coarse operating grid system (100~190NM) which does not allow sufficient resolution to describe adequately the resultant sea state in typhoon areas. Thus, TYWAVES, an improved model for typhoons with a locally finer grid, was developed by NEPRF. FNOC judged that TYWAVES is worthy of evaluation as a possible operational typhoon sea state model [14].

The TYWAVES is intended to produce fields of significant wave height and spectral wave properties on a mesh size consistent with the scales of tropical cyclones and is designed, primarily, for the application to the western North Pacific.

The detailed outputs of TYWAVES are in the form of fields, at each of 12 points, of spectral energy

components, significant wave heights, maximum wave periods, and the predominant wave directions, for 00, 12, 24, 48 and 72 hours, where 00 hours is the time of the first typhoon warning issued. An example of those outputs for Typhoon Owen is shown in Appendix A.

Using these spectral energy components at selected source points, I was able to make predictions based on the propagation of these components as swell into the region, south of Cheju-do, Korea (see Map I, page 21). More details of TYWAVES are described in Ref. 11.

D. FORECASTING AND VERIFICATION

Extremely high sea states are known to be generated in the quadrant to the right of the direction of movement of typhoons. The wave generation in that quadrant of the typhoon derived in TYWAVES from a spectral model utilizing the Pierson-Moskowitz (1964) spectrum. The model describes the spectroangular components of the waves present at a number of grid points in the region of strong winds. Each spectral component of interest is then permitted to propagate at its appropriate group velocity to the forecast site. The method is applied to three western North Pacific typhoons in 1979 and the forecast products are compared with the observed swell data from the south coastal area of Cheju-do, Korea.

TABLE 1.

WESTERN NORTH PACIFIC

1979 SIGNIFICANT TROPICAL CYCLONES

CYCLONE	TYPE	NAME	PERIOD OF WARNING	CALENDAR DAYS OF WARNING	MAX SFC WIND	MIN OBS SLP	NUMBER OF WARNINGS	DISTANCE TRAVELLED
01	TY	ALICE	01 JAN-14 JAN	14	110	930	51	2597
02	TY	BESS	20 MAR-25 MAR	6	90	958	21	1804
03	TY	CECIL	11 APR-20 APR	10	80	965	40	2535
04	TS	DOT	10 MAY-16 MAY	7	40	984	24	2876
05	TD	TD-05	23 MAY-24 MAY	2	30	998	6	2170
06	TY	ELLIS	01 JUL-06 JUL	6	85	955	22	1612
07	TS	FAYE	01 JUL-06 JUL	6	40	998	20	1837
08	TD	TD-08	24 JUL-25 JUL	2	20	1004	5	1264
09	ST	HOPE	27 JUL-03 AUG	10	130	898	33	3928
10	TS	GORDON	26 JUL-29 JUL	4	60	980	13	1058
11	TD	TD-11	03 AUG-06 AUG	4	25	997	14	1088
12	TY	IRVING	09 AUG-18 AUG	10	90	954	38	2732
13	ST	JUDY	16 AUG-26 AUG	11	135	887	39	2502
14	TD	TD-14	18 AUG-20 AUG	3	20	1006	9	605
15	TS	KEN	01 SEP-04 SEP	5	60	985	13	1418
16	TY	LOLA	02 SEP-08 SEP	7	90	950	23	1298
17	TY	MAC	15 SEP-24 SEP	10	70	984	35	1831
18	TS	NANLY	19 SEP-22 SEP	4	45	993	14	528
19	TY	OWEN	22 SEP-01 OCT	10	110	918	37	2151
20	TS	PAMELA	25 SEP-26 SEP	3	45	1002	6	984
21	TS	ROGER	03 OCT-07 OCT	6	45	985	16	1920
22	TY	SARAH	04 OCT-15 OCT	12	110	929	43	1194
23	ST	TIP	05 OCT-19 OCT	16	165	870	60	3972
24	ST	VERA	02 NOV-07 NOV	6	140	915	23	1868
25	TS	WAYNE	08 NOV-13 NOV	6	50	990	22	1559
26	TD	TD-26	01 DEC-02 DEC	2	30	998	6	1070
27	TY	ABBY	01 DEC-14 DEC	14	110	951	52	4044
28	TS	BEN	21 DEC-23 DEC	3	60	990	10	2245
1979 TOTALS				149*			695	

*OVERLAPPING DAYS INCLUDED ONLY ONCE IN SUM.

TABLE 2.

1979 SIGNIFICANT TROPICAL CYCLONE STATISTICS

WESTERN NORTH PACIFIC	JAN	FEB	MAR	APR	MAY	JUN	JUL	AUG	SEP	OCT	NOV	DEC	TOTAL	(1959-78) AVERAGE
TROPICAL DEPRESSIONS	0	0	0	0	1	0	1	2	0	0	0	1	5	4.8
TROPICAL STORMS	0	0	0	0	1	0	2	0	4	1	1	1	10	10.0
TYPHOONS	1	0	1	1	0	0	2	2	2	2	1	1	13	18.0
ALL CYCLONES	1	0	1	1	2	0	5	4	6	3	2	3	28	32.8
(1959-78) AVERAGE	0.6	0.4	0.6	0.9	1.4	2.1	5.2	6.8	6.0	4.8	2.7	1.3	32.8	

FORMATION ALERTS 23 of the 27 (85%) Formation Alert Events developed into tropical cyclones.
5 of the 28 (18%) tropical cyclones did not have a Formation Alert.

WARNINGS Number of warning days: 149
Number of warning days with 2 cyclones: 38
Number of warning days with 3 or more cyclones: 5

Figure 1. Typhoon tracks

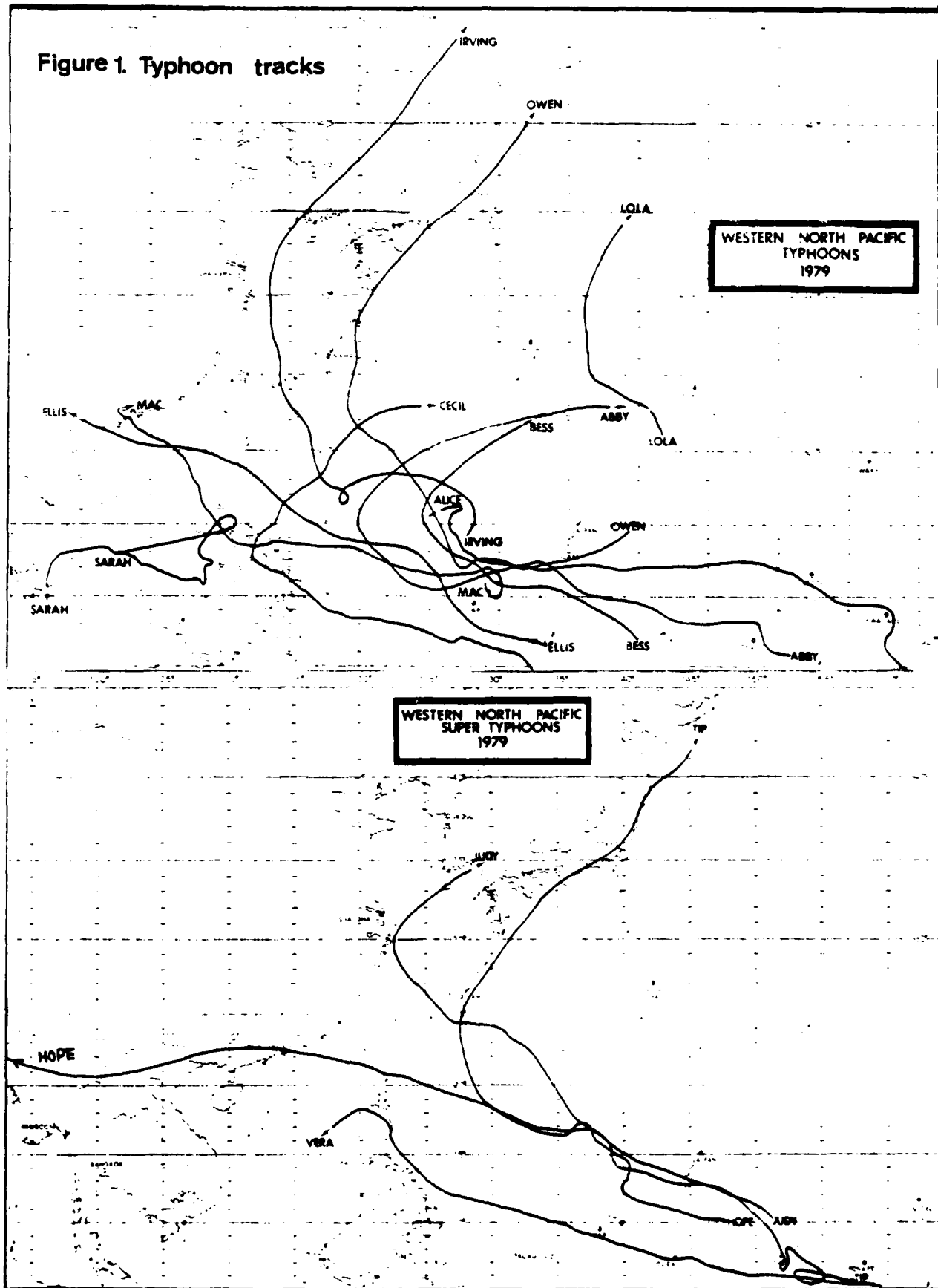
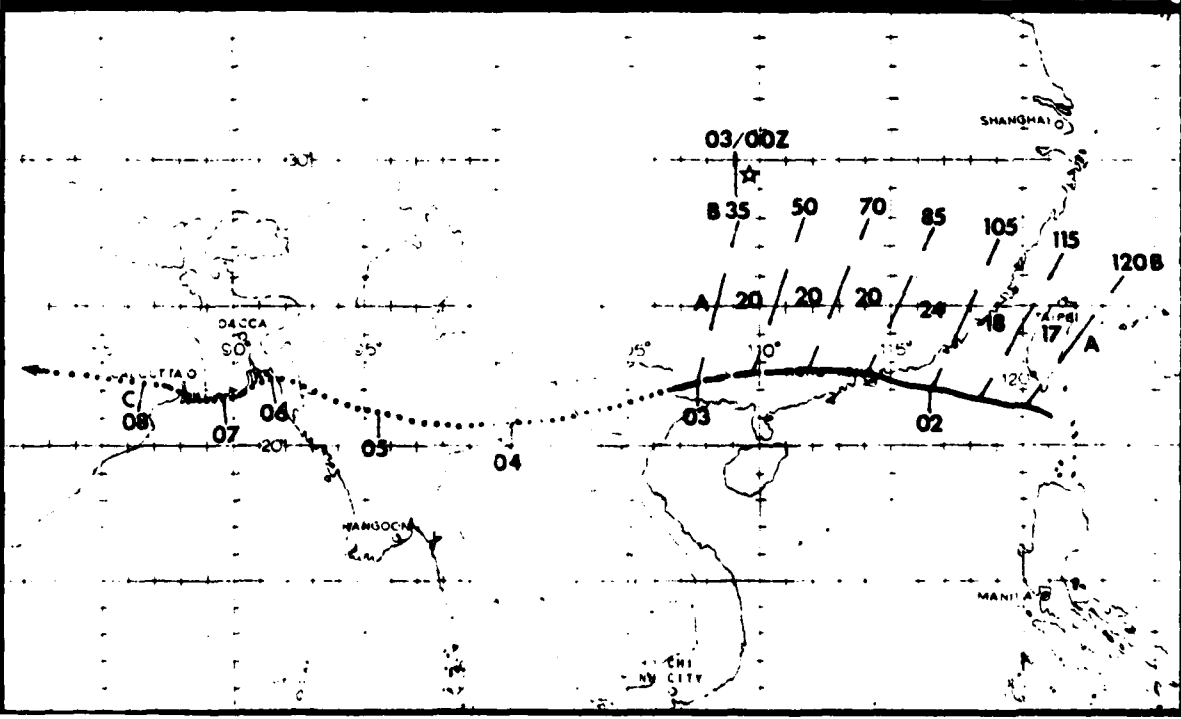
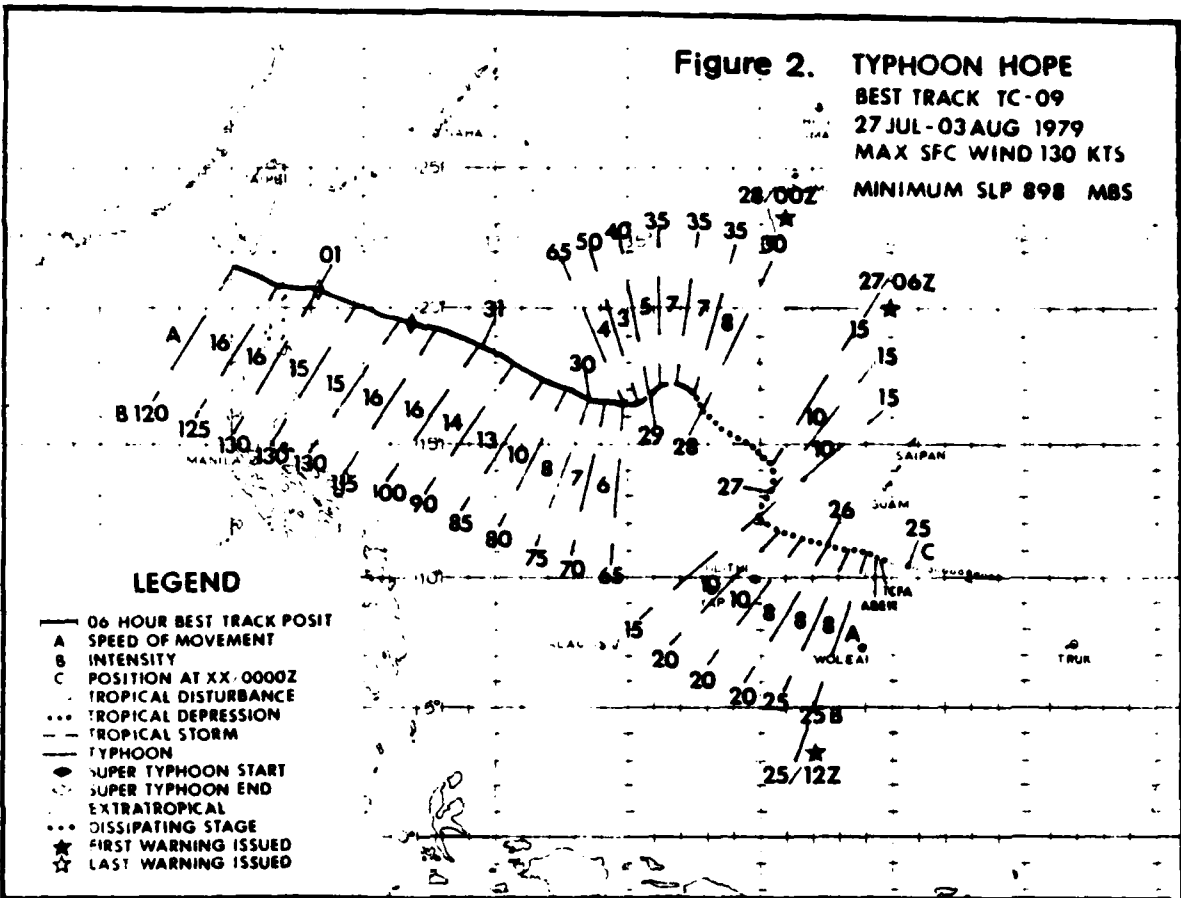


Figure 2. TYPHOON HOPE
BEST TRACK TC-09
27 JUL-03 AUG 1979
MAX SFC WIND 130 KTS
MINIMUM SLP 898 MBS



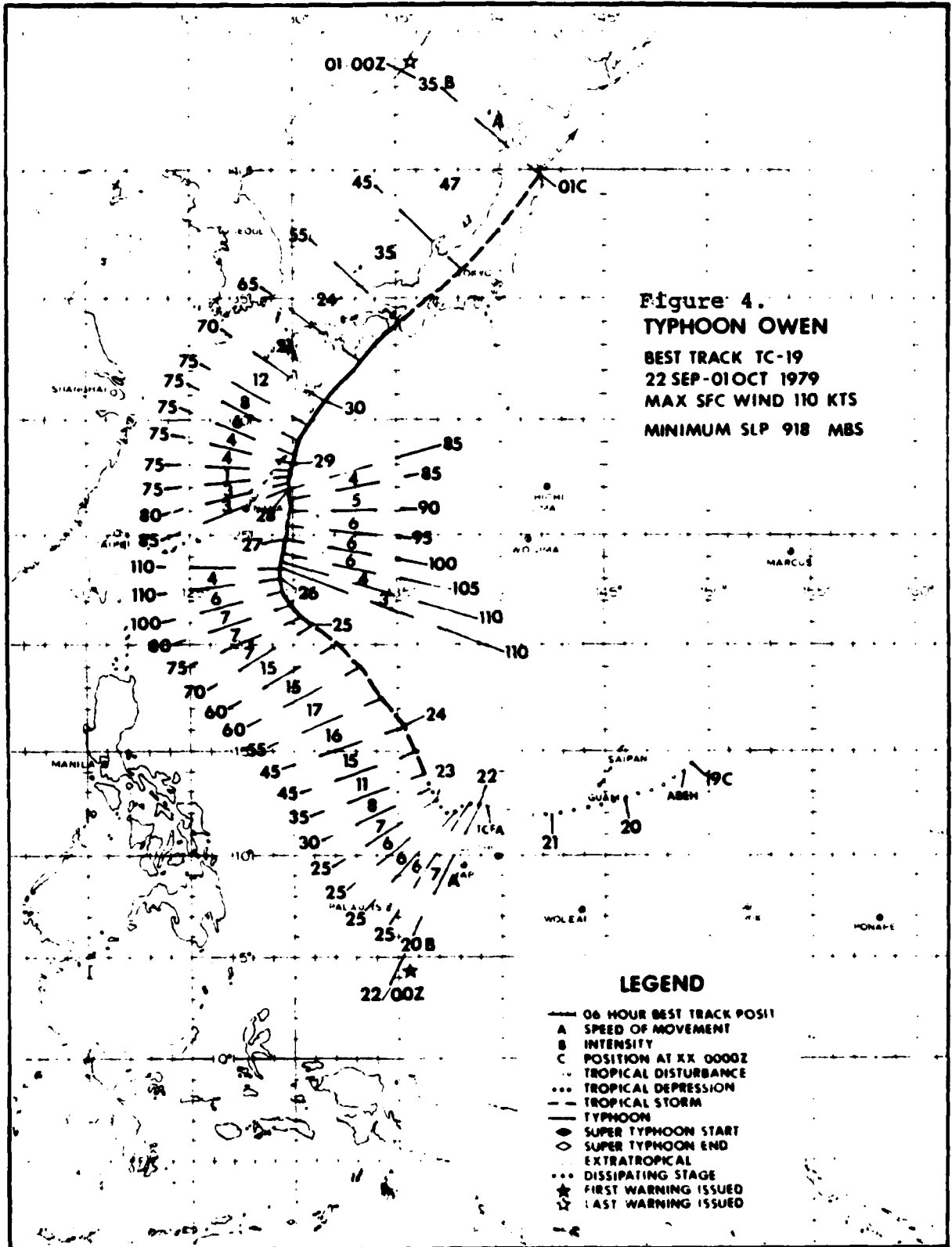


Figure 3.

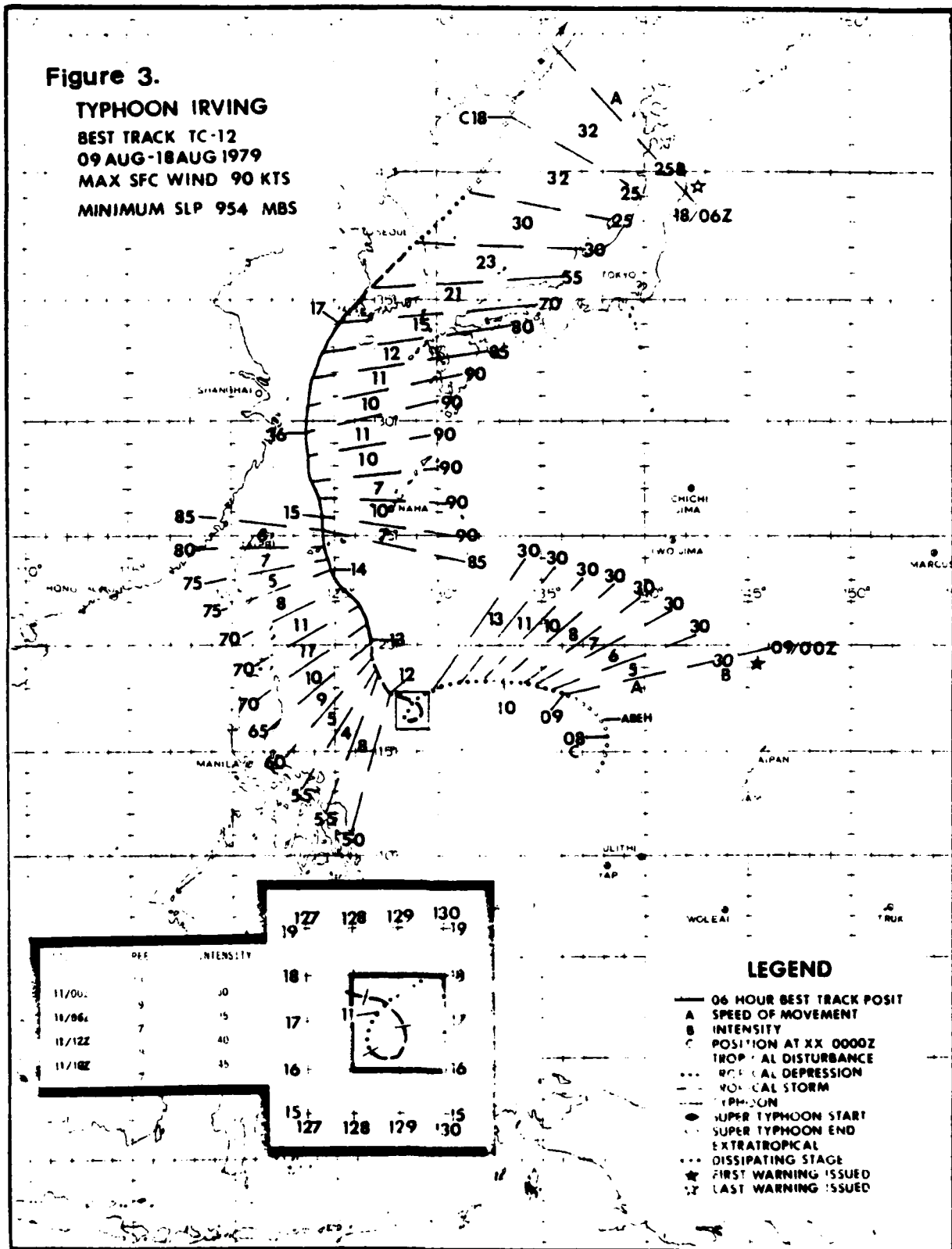
TYPHOON IRVING

BEST TRACK TC-12

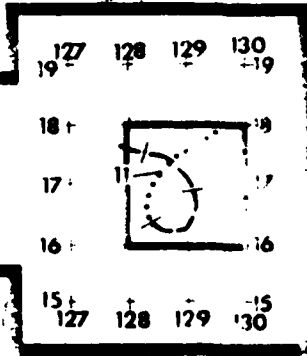
09 AUG-18 AUG 1979

MAX SFC WIND 90 KTS

MINIMUM SLP 954 MBS



DATE	INTENSITY
11/00Z	20
11/06Z	15
11/12Z	40
11/18Z	45



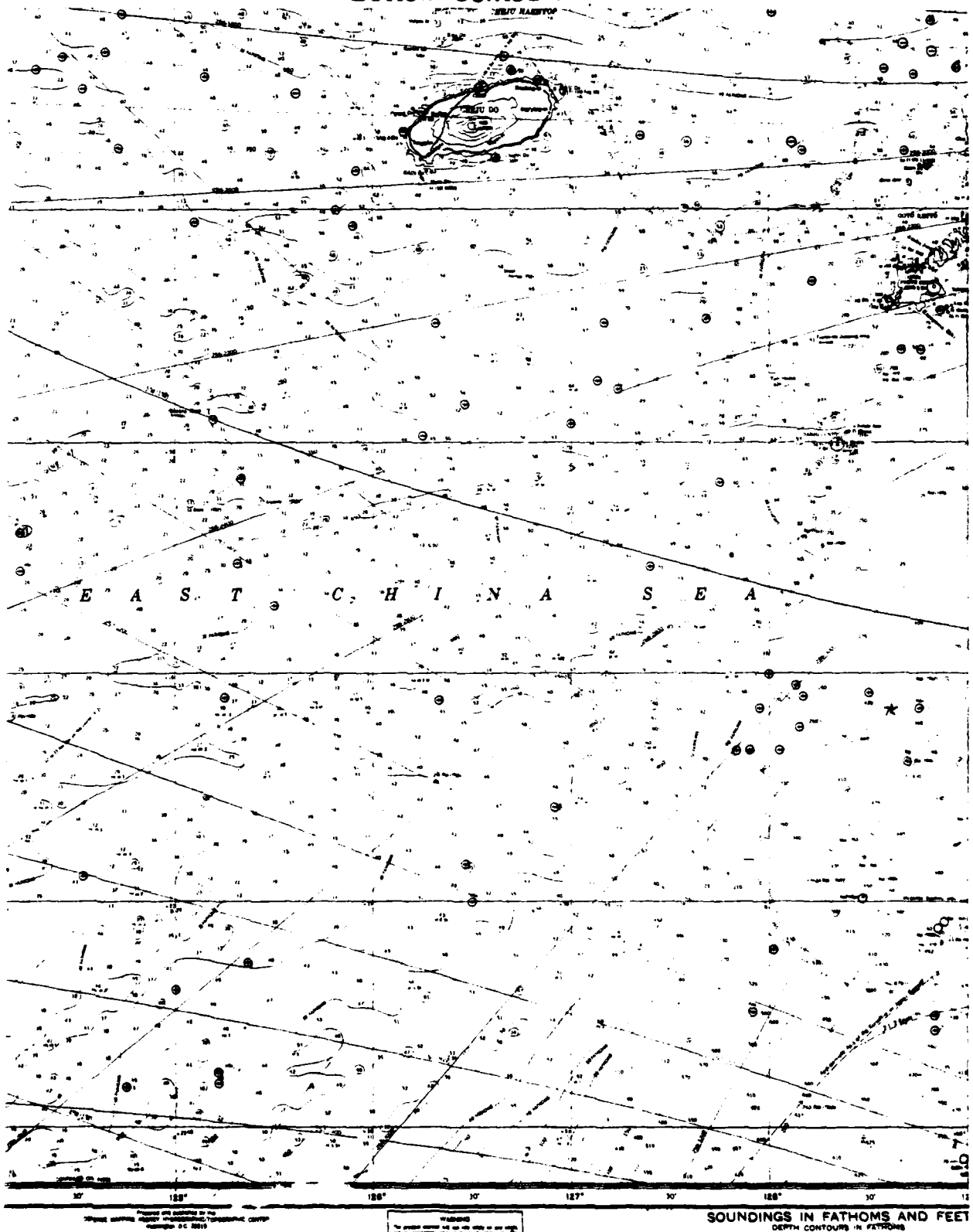
- LEGEND**
- 06 HOUR BEST TRACK POSIT
 - A SPEED OF MOVEMENT
 - B INTENSITY
 - C POSITION AT XX 0000Z
 - ... TROPICAL DISTURBANCE
 - TROPICAL DEPRESSION
 - TROPICAL STORM
 - TYPHOON
 - SUPER TYPHOON START
 - SUPER TYPHOON END
 - EXTRATROPICAL
 - ... DISSIPATING STAGE
 - ★ FIRST WARNING ISSUED
 - ☆ LAST WARNING ISSUED

Table 3. Best track

SUPER TYPHOON HOPE

BEST TRACK				WINDING				24 HOUR FORECAST				48 HOUR FORECAST				72 HOUR FORECAST					
NO/DATE	POSIT	WIND	DIR	POSIT	WIND	DIR	ERR	POSIT	WIND	DIR	ERR	POSIT	WIND	DIR	ERR	POSIT	WIND	DIR	ERR		
072007	10.2 147.4	20	0.0	0.0	U	-0.0	U	0.0	0.0	0	0	0.0	0.0	0	0	0.0	0.0	0	0		
072012	10.3 146.4	20	0.0	0.0	U	-0.0	U	0.0	0.0	0	0	0.0	0.0	0	0	0.0	0.0	0	0		
072018	10.3 146.2	20	0.0	0.0	U	-0.0	U	0.0	0.0	0	0	0.0	0.0	0	0	0.0	0.0	0	0		
072007	10.0 145.4	20	0.0	0.0	U	-0.0	U	0.0	0.0	0	0	0.0	0.0	0	0	0.0	0.0	0	0		
072007	10.7 144.8	24	0.0	0.0	U	-0.0	U	0.0	0.0	0	0	0.0	0.0	0	0	0.0	0.0	0	0		
072017	10.9 143.0	24	11.0	143.1	25	7	0	12.4	140.4	30	62	17.4	137.0	35	147	15	14.1	133.2	45	267	10
072010	11.1 141.1	24	11.1	141.0	25	14	0	12.7	134.4	30	142	17.4	130.4	35	240	10	14.0	118.3	45	341	10
072002	11.2 142.4	24	11.1	142.7	25	19	0	12.7	134.1	30	92	17.4	130.8	35	220	5	14.8	110.0	45	325	5
072004	11.5 141.4	24	11.6	141.4	20	4	0	12.7	137.4	30	171	17.4	133.0	35	240	0	14.2	124.2	45	340	-5
072017	11.8 140.7	24	11.4	140.4	20	4	0	13.0	137.0	30	192	17.4	132.7	35	300	0	14.7	128.5	45	345	-20
072012	12.3 139.4	14	12.0	139.7	20	13	5	13.4	134.7	30	199	17.4	131.0	35	305	0	14.7	127.0	45	317	-20
072002	13.2 140.1	14	12.7	139.7	20	66	5	14.4	134.0	25	174	17.4	131.0	35	240	-10	17.0	127.5	35	147	-40
072002	14.2 140.1	14	13.7	140.7	20	34	0	0.0	0.0	0	0	0.0	0.0	0	0	0.0	0.0	0	0	0	0
072012	15.0 139.4	20	0.0	0.0	U	-0.0	U	0.0	0.0	0	0	0.0	0.0	0	0	0.0	0.0	0	0	0	0
072012	15.0 138.4	24	0.0	0.0	U	-0.0	U	0.0	0.0	0	0	0.0	0.0	0	0	0.0	0.0	0	0	0	0
072002	15.0 138.4	24	0.0	0.0	U	-0.0	U	0.0	0.0	0	0	0.0	0.0	0	0	0.0	0.0	0	0	0	0
072002	16.1 137.4	30	16.2	137.4	25	4	-5	14.4	134.0	40	180	17.4	129.0	45	240	-25	20.3	129.2	40	241	-40
072007	16.0 137.4	34	17.5	138.4	25	85	-10	20.7	134.0	40	234	17.4	131.1	45	420	-30	24.3	129.0	40	340	-45
072017	17.2 136.0	34	18.2	137.2	25	62	-10	21.4	134.0	35	300	17.4	131.3	45	300	-40	24.8	127.2	35	370	-75
072017	17.1 135.2	34	14.4	136.0	25	110	-10	22.2	134.4	35	311	17.4	129.0	45	407	-45	24.0	123.3	35	402	-75
072002	16.7 135.7	40	16.4	135.2	30	23	-5	17.4	137.2	30	80	17.4	128.0	40	40	-40	19.4	126.1	40	95	-45
072002	16.0 135.4	40	16.2	135.1	40	23	-10	16.2	137.4	30	50	17.1	130.1	40	185	-35	14.0	127.2	40	161	-40
072012	16.0 134.0	44	16.4	134.0	45	0	0	17.1	137.4	35	30	17.4	129.3	45	192	-45	20.3	123.7	45	321	-20
072012	16.7 134.2	44	16.4	134.4	40	14	0	17.3	131.4	40	80	17.4	128.7	45	240	-45	20.6	123.1	45	300	-20
072002	16.0 133.4	44	16.4	133.4	45	4	0	18.0	134.2	40	110	17.4	128.9	45	210	-30	20.0	122.4	45	340	-40
072007	17.1 132.7	44	17.4	132.4	40	4	0	18.2	129.4	40	121	17.4	128.3	45	240	-25	21.0	122.1	45	470	15
072012	17.0 131.4	44	17.2	132.4	40	17	5	18.1	124.1	40	147	17.4	125.0	45	180	0	21.0	121.8	45	440	40
072012	18.0 130.4	44	17.5	131.1	45	41	5	19.0	124.0	40	147	17.4	124.0	45	180	5	21.3	120.8	45	425	40
072002	18.0 129.4	44	18.5	129.3	40	4	0	20.4	124.0	40	140	17.4	120.0	45	200	-5	21.8	115.2	45	427	40
072002	19.3 127.4	44	19.2	128.4	40	11	-10	21.7	123.2	40	104	17.4	117.9	45	222	-5	21.8	113.8	25	470	-40
072012	19.0 126.2	44	19.7	126.4	40	11	0	21.4	124.1	40	104	17.4	115.7	45	211	-35	20.0	110.0	40	400	0
072012	20.1 124.7	44	20.1	124.4	40	6	0	22.0	114.4	40	29	17.4	113.1	45	133	-25	20.0	108.0	40	400	0
072002	20.0 123.2	44	20.7	123.2	40	4	0	22.4	117.2	40	54	17.4	110.0	45	0	0	20.0	108.0	40	400	0
072002	20.0 123.2	44	20.7	123.2	40	4	0	22.4	117.2	40	54	17.4	110.0	45	0	0	20.0	108.0	40	400	0
072002	20.0 123.2	44	20.7	123.2	40	4	0	22.4	117.2	40	54	17.4	110.0	45	0	0	20.0	108.0	40	400	0
072002	20.0 123.2	44	20.7	123.2	40	4	0	22.4	117.2	40	54	17.4	110.0	45	0	0	20.0	108.0	40	400	0
072002	20.0 123.2	44	20.7	123.2	40	4	0	22.4	117.2	40	54	17.4	110.0	45	0	0	20.0	108.0	40	400	0
072002	20.0 123.2	44	20.7	123.2	40	4	0	22.4	117.2	40	54	17.4	110.0	45	0	0	20.0	108.0	40	400	0
072002	20.0 123.2	44	20.7	123.2	40	4	0	22.4	117.2	40	54	17.4	110.0	45	0	0	20.0	108.0	40	400	0
072002	20.0 123.2	44	20.7	123.2	40	4	0	22.4	117.2	40	54	17.4	110.0	45	0	0	20.0	108.0	40	400	0
072002	20.0 123.2	44	20.7	123.2	40	4	0	22.4	117.2	40	54	17.4	110.0	45	0	0	20.0	108.0	40	400	0
072002	20.0 123.2	44	20.7	123.2	40	4	0	22.4	117.2	40	54	17.4	110.0	45	0	0	20.0	108.0	40	400	0
072002	20.0 123.2	44	20.7	123.2	40	4	0	22.4	117.2	40	54	17.4	110.0	45	0	0	20.0	108.0	40	400	0
072002	20.0 123.2	44	20.7	123.2	40	4	0	22.4	117.2	40	54	17.4	110.0	45	0	0	20.0	108.0	40	400	0
072002	20.0 123.2	44	20.7	123.2	40	4	0	22.4	117.2	40	54	17.4	110.0	45	0	0	20.0	108.0	40	400	0
072002	20.0 123.2	44	20.7	123.2	40	4	0	22.4	117.2	40	54	17.4	110.0	45	0	0	20.0	108.0	40	400	0
072002	20.0 123.2	44	20.7	123.2	40	4	0	22.4	117.2	40	54	17.4	110.0	45	0	0	20.0	108.0	40	400	0
072002	20.0 123.2	44	20.7	123.2	40	4	0	22.4	117.2	40	54	17.4	110.0	45	0	0	20.0	108.0	40	400	0
072002	20.0 123.2	44	20.7	123.2	40	4	0	22.4	117.2	40	54	17.4	110.0	45	0	0	20.0	108.0	40	400	0
072002	20.0 123.2	44	20.7	123.2	40	4	0	22.4	117.2	40	54	17.4	110.0	45	0	0	20.0	108.0	40	400	0
072002	20.0 123.2	44	20.7	123.2	40	4	0	22.4	117.2	40	54	17.4	110.0	45	0	0	20.0	108.0	40	400	0
072002	20.0 123.2	44	20.7	123.2	40	4	0	22.4	117.2	40	54	17.4	110.0	45	0	0	20.0	108.0	40	400	0
072002	20.0 123.2	44	20.7	123.2	40	4	0	22.4	117.2	40	54	17.4	110.0	45	0	0	20.0	108.0	40	400	0
072002	20.0 123.2	44	20.7	123.2	40	4	0	22.4	117.2	40	54	17.4	110.0	45	0	0	20.0	108.0	40	400	0
072002	20.0 123.2	44	20.7	123.2	40	4	0	22.4	117.2	40	54	17.4	110.0	45	0	0	20.0	108.0	40	400	0
072002	20.0 123.2	44	20.7	123.2	40	4	0	22.4	117.2	40	54	17.4	110.0	45	0	0	20.0	108.0	40	400	0
072002	20.0 123.2	44	20.7	123.2	40	4	0	22.4	117.2	40	54	17.4	110.0	45	0	0	20.0	108.0	40	400	0
072002	20.0 123.2	44	20.7	123.2	40	4	0	22.4	117.2	40	54	17.4	110.0	45	0	0	20.0	108.0	40	400	0
072002	20.0 123.2	44	20.7	123.2	40	4	0	22.4	117.2	40	54	17.4	110.0	45	0	0	20.0	108.0	40	400	0
072002	20.0 123.2	44	20.7	123.2	40	4	0	22.4	117.2	40	54	17.4	110.0	45	0	0	20.0	108.0	40	400	0
072002	20.0 123.2	44	20.7	123.2	40	4	0	22.4	117.2	40	54	17.4	110.0	45	0	0	20.0	108.0	40	400	0
072002	20.0 123.2	44	20.7	123.2	40	4	0	22.4	117.2	40	54	17.4	110.0	45	0	0	20.0	108.0	40	400	0
072002	20.0 123.2	44	20.7	123.2	40	4	0	22.4	117.2	40	54	17.4	110.0	45	0	0	20.0	108.0	40	400	0
072002	20.0 123.2	44	20.7	123.2	40	4	0	22.4	117.2	40	54	17.4	110.0	45	0	0	20.0	108.0	40	400	0
072002	20.0 123.2	44	20.7	123.2	40	4	0	22.4	117.2	40	54	17.4	110.0	45	0	0	2				

MAP 1. East China Sea Bottom Contours



The dispersive arrival at the prediction site of the waves propagating from a single source region is represented by a plot of period versus arrival time in Figures 9, 10 and 11. The energy in each low frequency (7~19 sec) spectral component of the swell at Cheju-do is calculated by modifying the energy spectrum at the source for the refraction and shoaling. The lowest period ($\bar{T} = 4$ sec) is assumed totally eliminated by attenuation.

The total propagated energy at any given time is estimated by summing all the directional components. The predicted swell heights $H_{1/10}$ are assumed to be related to the energy by $H_{1/10} = K\sqrt{E}$, where K is constant (0.4) and E is energy in a unit of 2^6 kiloerg/cm² and $H_{1/10}$ is in meters.

By graphing the energy associated with the 5 mean period bands as a function of arrival time at the forecast site and summing, then a plot of the total propagated energy is obtained (see Figures 13, 15 and 17). This plot is compared with the observed wave heights in Chapter IV-D.

E. TERMINOLOGY

To make clear the notation used in this study, the following terms and symbols are defined.

- sea - Those waves found within a generating area.
- swell - Those waves which have moved out of a generating area.
- R_0 - The distance from the source to the "bottom line" where the corresponding periods feel "bottom" i.e., the swell travel distance in deep water. The depth at the "bottom line" is $h = \frac{L_0}{2}$.
- R - The distance from the "bottom line" to the forecast site.
- \bar{T} - The mean period in a spectral band ($\bar{T} = 1/\bar{f}$).
- H_{1/10} - The average heights of the 1/10 highest waves.
- H_{1/3} - The average heights of the 1/3 highest waves (significant wave height).
- tar - The swell arrival time (GMT).
- t - The swell travel time.
- L - Wavelength (L_0 in deep water).
- C_g - Group velocity (C_{g_0} in deep water).
- C - Phase speed (C_0 in deep water).
- D - The total swell travel distance ($D = R_0 + R$).
- g - Acceleration of gravity
- σ - Wave angular frequency ($2\pi/L$).
- k - Wave number ($2\pi/L$).
- h(d) - The water depth.

- α_0 - The angle between wave crest and bottom contour at the depth, $h = \frac{L_0}{2}$.
- T_4 - The total energy at grid point 4 in the generating area.
- D_4 - The directional energy component at grid point 4 in generating area.

Wave spectrum (energy spectrum) - The distribution of either wave height or energy with period. The potential energy of the sea surface is proportional to the mean of the square of the wave height.

Dispersion - A process which leads to longitudinal spreading of the wave energy as, in deep water, energy in each spectral component is propagated at a characteristic group velocity C_g , the long waves having the larger group velocity.

- $\bar{\theta}$ - The mean directional bands of 16 unit points rose.
- H'_0 - The wave height before refraction in deep water.

II. PREDICTION OF TROPICAL STORM WAVES BY TYWAVES

A. LOCATION OF THE SELECTED POINT-SOURCES

The TYWAVES program produces a printout of the complete energy spectrum for 12 points around each typhoon. Each point lies at a chosen distance from the storm center in a fixed direction, no matter what the storm movement direction is. These points are representative origins of the wave energy emerging from the typhoon.

Only those points are selected which are in the region of maximum winds and where important energy components are directed toward the distant prediction site.

The arrangement of points whose wave spectra are used in this study is shown below.

			+9		
		+5	+1	+6	
+11	+3	+1	+4	+12	
		+7	+2	+8	
			+10		

The distances from the storm center to points 1, 2, 3 and 4 are three grid-lengths ($3 \times 40 = 120$ NM), to 9, 10, 11 and 12 are five grid lengths ($5 \times 40 = 200$ NM), and to

5, 6, 7 and 8 are $3 \times \sqrt{2}$ grid lengths ($3 \times \sqrt{2} \times 40 \approx 170$ NM), respectively.

Among the 12 points, only points 4, 6, 8 and 12 were selected as sources, because the spectral energy from only these 4 points can propagate to Cheju-do, Korea (33.2°N 126.6°E).

The locations of the sources for each time of interest for the three storms are shown below in Table VI, which was derived and calculated from the postanalysis "best track" data shown in Tables III, IV, and V [2]. The relationship between latitude and longitude is:

$$\begin{aligned} \text{Lat.} &= \text{Long.} \times \cos (\text{Lat.}) \\ &= \text{Long.} \times \cos \left\{ \frac{(\text{storm center} + \text{forecast})}{2} \right\} \\ &\quad \text{lat} \end{aligned}$$

e.g.:

When the storm center (best track) is 20.0°N 126.7°E , point 4 is same lat (20.0°N), but 120 NM (2° in lat) east of the center.

$$\begin{aligned} \text{Thus, } 2^{\circ} \text{ Lat} &= \text{Long} \times \cos \left(\frac{20.0 + 20.0}{2} \right) \\ &= \text{Long} \times \cos 10^{\circ} \end{aligned}$$

$$\begin{aligned} \therefore \text{Long} &= 2^{\circ} \text{ Lat} / \cos 10^{\circ} = 2.128^{\circ} \text{ E} \\ &= 126.7 + 2.128 \\ &= 128.8^{\circ} \text{ E} \end{aligned}$$

Therefore, point 4 $\approx 20.0^{\circ}\text{N}$ 128.8°E .

TABLE 6

Typhoon Centers and Selected Points Location

Name	Date (GMT)	Center (°N-°E)	PT4 (°N-°E)	PT6 (°N-°E)	PT8 (°N-°E)	PT12 (°N-°E)
HOPE	073012	17.4-131.8	17.4-133.9	19.4-133.9	15.4-133.9	17.4-135.3
	073100	18.6-129.4	18.6-131.5	20.6-131.5	16.6-131.5	18.6-132.9
	073112	19.6-126.2	19.6-128.3	21.6-128.3	17.6-128.3	19.6-129.7
	080100	20.6-123.2	20.6-125.3	22.6-125.4	18.6-125.3	20.6-126.8
	080112	21.5-120.1	21.5-122.2	23.5-122.3	19.5-122.2	21.5-123.7
	081300	20.0-126.7	20.0-128.8	22.0-128.8	18.0-128.8	20.0-130.2
IRVING	081312	22.0-126.0	22.0-128.2	24.0-128.2	20.0-128.1	22.0-129.6
	081400	23.5-125.0	23.5-127.2	25.5-127.2	21.5-127.2	23.5-128.6
	081412	24.6-124.5	24.6-126.7	26.6-126.7	22.6-126.7	24.6-128.2
	081500	25.9-124.3	25.9-126.5	27.9-126.5	23.9-126.5	25.9-128.0
	081512	27.5-123.7	27.5-126.0	29.5-126.0	25.5-125.9	27.5-127.5
	081600	29.6-123.7	29.6-126.0	31.6-126.0	27.6-126.0	29.6-127.5
	081612	31.7-123.7	31.7-126.1	33.7-126.1	29.7-126.1	31.7-127.6
	092506	21.3-130.3	21.3-132.4	23.3-132.5	19.3-132.4	21.3-133.9
	092518	22.6-129.5	22.6-131.7	24.6-131.7	20.6-131.7	22.6-133.1
	092606	23.5-129.2	23.5-131.4	25.5-131.4	21.5-131.4	23.5-132.8
OWEN	092618	24.4-129.4	24.4-131.6	26.4-131.6	22.4-131.6	24.4-133.3
	092706	25.5-129.7	25.5-131.9	27.5-131.9	23.5-131.9	25.5-133.4
	092718	26.5-129.8	26.5-131.9	28.5-132.1	24.5-132.0	26.5-133.5
	092806	27.3-129.8	27.3-132.1	29.3-132.1	25.3-132.0	27.3-133.5
	092818	27.8-129.8	27.8-132.1	29.8-132.1	25.8-132.0	27.8-133.6
	092906	28.5-130.1	28.5-132.4	30.5-132.4	26.5-132.4	28.5-133.9
	092918	29.8-130.6	29.8-132.9	31.8-132.9	27.8-132.9	29.8-134.4

B. SEA-SPECTRA AT THE POINT SOURCES

The description of the wave fields using the spectral component method developed by NEPRF was used in this study. Only those directional components able to propagate to the forecast site need be considered.

A schematic example of the TYWAVES spectral prediction in a typhoon area is given below. The whole spectral table for the selected sources is shown in Appendix B.

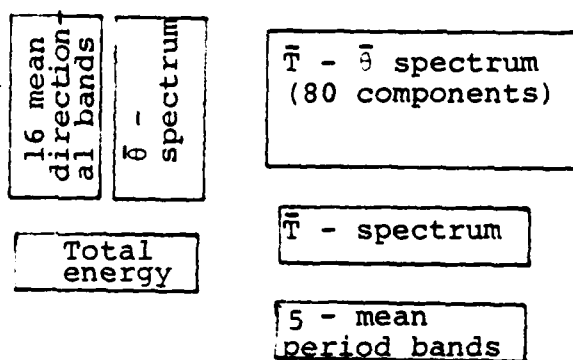


Table VII is one example of a period-direction spectrum at source point 4 in Typhoon Owen, at 06 on 25 September 1979.

The mean period is 13 sec with the maximum energy 86 (2^6 kiloeng/cm²) in the dominant period. The dominant wave direction is SE, but the energy from that direction will not arrive at the forecast site, only the SSE component will arrive at the site (as seen in Figure 5).

C. SELECTION OF THE DIRECTIONAL ENERGY AT POINT SOURCES

A constant energy was assumed between parallel rays separated by width 80-160 NM (2-4 grid length), which is 40-80 NM right at the grid point depending upon the typhoon size. This is why the energy in each component is assumed constant along the deep water propagation path. As example of possible refraction diagrams under the above consideration and bottom contours in Map 1 is shown in Figure 5.

Only the SSE component was considered to propagate to the forecast site. The SE component would refract toward China, west of Cheju-do, and the S component would pass to the east of Cheju-do as seen in Figure 5.

All the directional components were chosen in the same way, and are underlined as shown in Table 7.

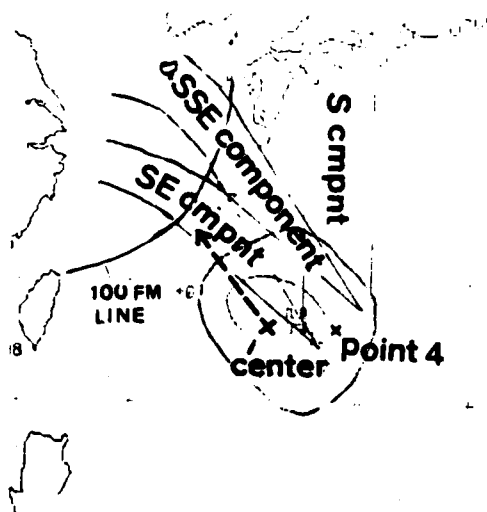


Figure 5. Possible refraction diagram at point 4 at 06 GMT September 25, 1979. The curves around typhoon center are contours of wave height ($H \frac{1}{3}$ in feet). The detailed bottom contours are shown on Map 1.

TABLE 7

Period-Directional Spectrum at Point 4 at 06 GMT September 25, 1979. The energy units are 2^6 kiloerg/cm².

TYPHOON WAVES POINT 4

H_{1/10} = 6.1 M

NORTH-CORRESPONDS TO THE AZIMUTH 360

N	0 *	0	0	0	0	0	0	
NNE	0 *	0	0	0	0	0	0	
NE	0 *	0	0	0	0	0	0	
ENE	0 *	0	0	0	0	0	0	
E	1 *	0	0	0	0	0	0	
ESE	32 *	0	6	6	17	1	0	
SE	93 *	0	8	25	27	24	8	
SSE	74 *	0	7	25	31	4	0	
S	31 *	0	4	10	10	4	2	
SSW	0 *	0	0	0	0	0	0	
SW	0 *	0	0	0	0	0	0	
WSW	0 *	0	0	0	0	0	0	
W	0 *	0	0	0	0	0	0	
WNW	0 *	0	0	0	0	0	0	
NW	0 *	0	0	0	0	0	0	
NNW	0 *	0	0	0	0	0	0	
TOTAL		232	0	26	69	36	10	
PERIODS			4	7	10	13	16	19

D. TOTAL AND DIRECTIONAL ENERGIES AT POINT SOURCES

Figures 6, 7 and 8 show the energy components at each selected grid point in the typhoon area. Each line is labeled by selected grid point (source point). T_n indicates total energy given by TYWAVES at point n and D_n represents the sum over all periods of the energies with proper direction to reach Cheju-do.

$$D_n(\theta_o) = \sum_{i=1}^{19} E_i(\bar{T}_i, \theta_o)$$

For example, where $n = 12$, θ is SE, then

$$\begin{aligned} D_{12}(\theta=SE) &= E_7(\bar{T}=4, \theta_o=SE) + E_{10}(\bar{T}=10, \theta_o=SE) \\ &+ E_{13}(\bar{T}=13, \theta_o=SE) + E_{16}(\bar{T}=16, \theta_o=SE) \\ &+ E_{19}(\bar{T}=19, \theta_o=SE). \end{aligned}$$

This represents the total energy at point 12 directed from SE toward Cheju-do.

The energy is in practice converted into height H 1/10 by making H 1/10 = $0.4 \sqrt{E}$, which is described in Chapter I.D. Some special features of the wave fields in each source are now discussed.

1. Typhoon Hope

The maximum sustained wind speed was over 100 kts for two days from 00 GMT July 31. The maximum wave height (H 1/10) recorded was 12.80 m. The directional energy components from grid point 12 were ignored from 00 GMT July 31 to 00 GMT August 01, because they were too small.

2. Typhoon Irving

Only the propagation of energy components until 00 GMT August 16 was considered, because the forecast site is inside of typhoon area after that time. Therefore, after 00 GMT August 16, the propagated wave energy should be combined with local energy at prediction site.

Among the directional components, only those from grid points 4 and 12 were propagated to the prediction site during the typhoon period, because the energies from other sources were refracted away from Cheju-do.

3. Typhoon Owen

After 06 GMT September 29, the typhoon passed east of southern Japan. No further propagation to Cheju-do occurred.

In most cases, only one directional energy component was selected at each grid point. But both components (SE and SSE) were able to reach the forecast site on 18 GMT September 27, from grid point 4, because of the width of their ray boundaries at distances near the source.

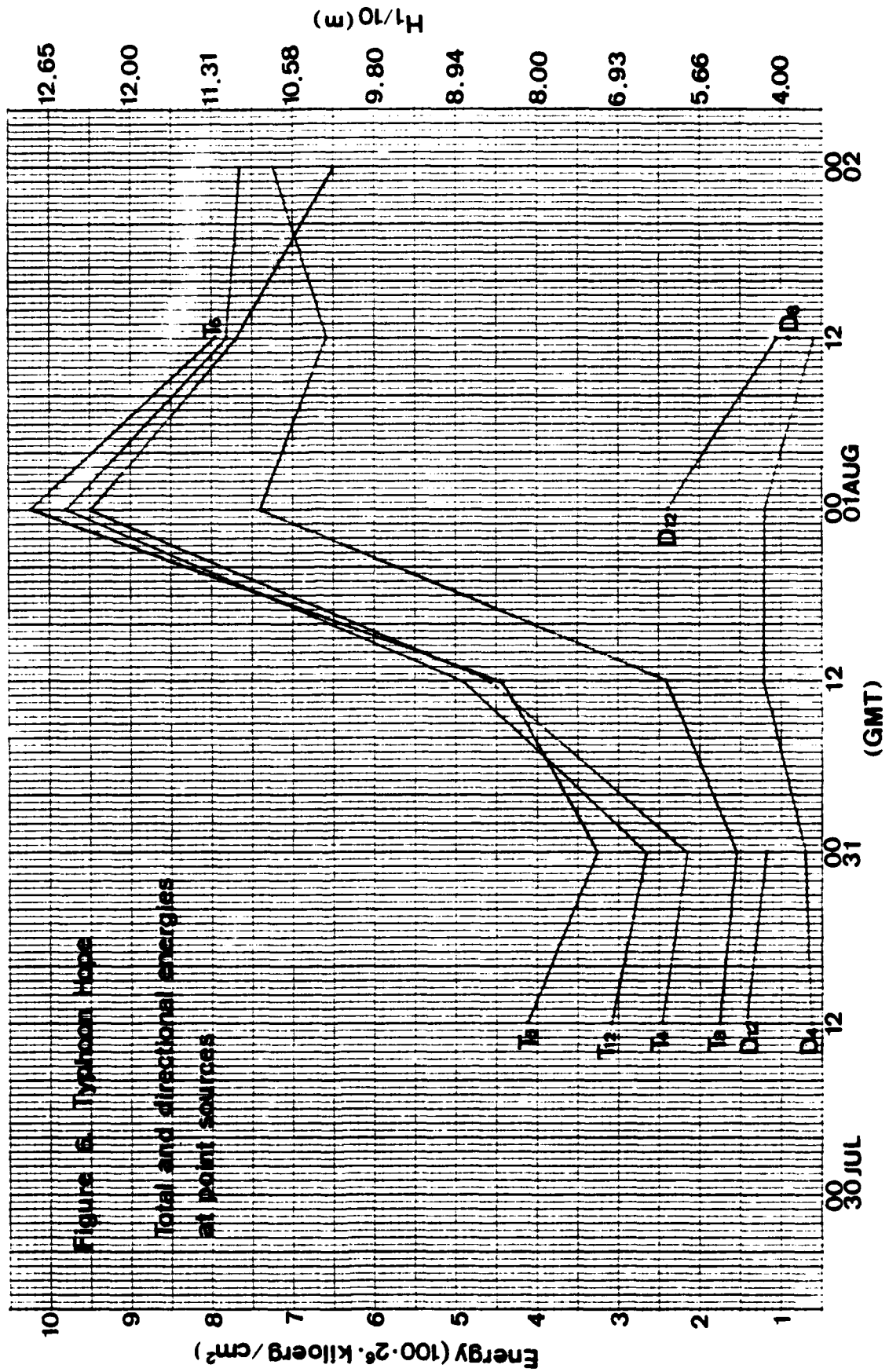
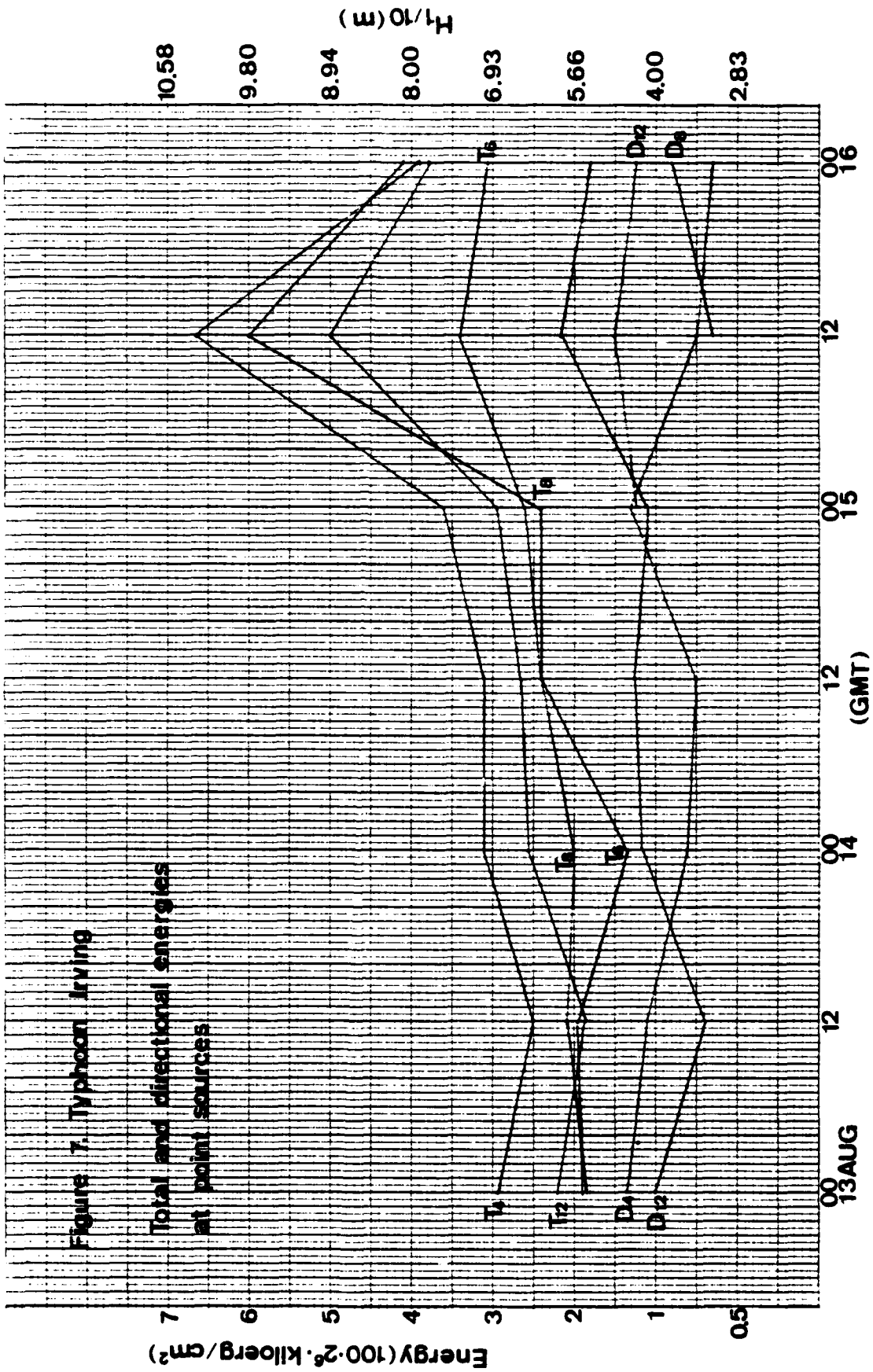


Figure 7. Typhoon Irving

Total and directional energies
at point sources



III. PREDICTION OF SWELL CHARACTERISTICS

The periods of high waves due to typhoons are usually in the range of 7-19 sec. They travel in deep water with the group corresponding velocities 10-30 kts. It normally necessitates 1-4 days for conspicuous swells generated in a typhoon in the far south seas to reach Cheju-do, Korea.

The group velocities of periods 7 and 10 sec are constant along their paths since they remain in "deep water." But for periods 13, 16 and 19 sec, the group velocities vary because of depth variations. Thus, I considered two distance components: in deep water R_0 and in shallow water R for periods 13, 16 and 19 sec.

The travel distances between grid points and observation points are calculated with the assumption of plane geometry. Then, group velocities, travel distances and travel times are derived for each period in this section.

A. THE SETTING OF THE FORECAST SITE AND ITS RELATION TO THE WAVE SOURCES

The passes of the Ryukyu Islands act as windows between the energy sources and the forecast site, Cheju-do, Korea. Since the largest land length for blockage of energy is only about 40 NM, this length is not sufficient to interrupt totally the energy propagation. Thus, as a further simplification, I neglected the effect of the Ryukyu Islands

against the energy propagation. The window is assumed sufficient for total propagation.

B. GROUP VELOCITY

Some simplifications are used in assigning group velocity values along the route from typhoons to the observation site.

From linear wave theory group velocity, C_g is given by

$$C_g = \frac{1}{2} \left[c + \frac{2kh}{\sinh 2kh} \right] = nc$$

(all the symbols are defined below)

and phase speed c is given by $c = \frac{g}{\sigma} \tanh kh$. In deep water this is well approximated by $c_0 = g/\sigma = 3.03 T$ (kts) for T given in seconds, and in shallow by $c = \sqrt{gh}$. But in the general case c varies with both the depth of water and the wavelength.

The classifications "deep" and "shallow" are given in terms of "relative depth h/L_0 ", described below. Since there is no "shallow water" between the wave sources and Cheju-do, Korea, (corresponding to the periods used by TYWAVES), I will use only the general equation and the deep water approximation. In these equations

C_g = group velocity

c = phase speed (c_0 in deep water)

n = the fraction of energy propagated at phase speed

g = gravity acceleration

h = water depth

σ = wave angular frequency ($2\pi/T = 2kf$, where T is period)

k = local wave number ($2\pi/L$, where L is wave length)

f = wave frequency ($1/T$)

It is important to note that c and group velocity, C_g must be found as functions of both h and σ . A straightforward method is illustrated below, where the dependence on kh is replaced by the deep water wavelength $L_0 = 2\pi g/\sigma^2$.

The local wavelength is then found from L/L_0 , a function of the relative depth h/L_0 .

Since $C/C_0 = L/L_0$, the phase speed c can be found from h and σ .

To estimate the group velocity by definition, $C_g = \frac{1}{2} c [1 + \frac{2kh}{\sinh kh}] = nc$ where, n takes on the following values for corresponding h/L_0 :

general case ($\frac{1}{2} \geq h/L_0 \geq \frac{1}{20}$): $1 > n > \frac{1}{2}$,

deep water case ($h/L_0 > \frac{1}{2}$): $n = \frac{1}{2}$.

In order to simplify calculations, I used $n = 3/4$ in the waters between the Ryukyu Islands and Cheju-do where, for the longer periods, the relative depth range $\frac{1}{2} \geq h/L_0 \geq \frac{1}{20}$. With this simplification, the corresponding group velocities become the following:

$$\bar{T} = 13 \text{ sec}; C_g = 29.4 \text{ kts}$$

$$\bar{T} = 16 \text{ sec}; C_g = 33.6 \text{ kts}$$

$$\bar{T} = 19 \text{ sec}; C_g = 35.8 \text{ kts}$$

The influence on the calculation of C_g of the use of these representative constant values is discussed in Chapter IV.D.

For deep water

$$C_o = 3.03T \text{ (kts for } T \text{ in sec)}$$

$$C_{g_o} = nc = \frac{1}{2} C_o = 1.515T \text{ (kts for } T \text{ in sec)}$$

Therefore, group velocity in knots and depth at which C_g replaces C_{g_o} are shown below:

\bar{T} (sec)	7	10	13	16	19
C_{g_o}/C_g (kts)	10.6/-	15.2/-	18.7/29.6	24.3/33.6	28.8/35.8
$h(\frac{L_o}{2}$ in ft)	126	256	433	656	924

C. TRAVEL DISTANCE AND ARRIVAL TIME

The travel distance between grid points in the storm and the observation point $33.2^{\circ}\text{N } 126.6^{\circ}\text{E}$ are calculated with the assumptions of plane geometry. Consider this example.

On 12 GMT July 30, the grid point 4 was at $17.4^{\circ}\text{N } 133.9^{\circ}\text{E}$.

Thus, the north-south component is given by

$$\begin{aligned}
 y &= [\text{lat (site)}^\circ - \text{lat (grid point)}^\circ] \times 60 \text{ NM} \\
 &= [33.2 - 17.4] \times 60 \\
 &= 948 \text{ NM}
 \end{aligned}$$

and the east-west component is approximated by

$$\begin{aligned}
 x &= [\text{long (grid point)} - \text{long (site)}] \cos (\text{mean lat}) \\
 &\quad \times 60 \text{ NM} \\
 &= [133.9 - 126.6] \cos (17.4) \times 60 \text{ NM} \\
 &= 418 \text{ NM}
 \end{aligned}$$

Thus, the travel distance, D, is given by

$$\begin{aligned}
 D &= (x^2 + y^2)^{\frac{1}{2}} \text{ and for grid point 4,} \\
 D &= (418^2 + 948^2)^{\frac{1}{2}} = 1036 \text{ NM}
 \end{aligned}$$

The travel time, t, is given by

$$t = \frac{R_0}{C_{g_0}} + \frac{R}{C_g}, \text{ where } R_0 + R = D$$

R_0 = the deep water distance

R = the remaining distance

Therefore, the arrival time, t_{ar} of each period band is given by

$$\begin{aligned}
 t_{ar} (\bar{T}) &= t_0 + t, \text{ where } t_0 = \text{leaving time from} \\
 &\quad \text{typhoon area} \\
 t &= \text{travel time}
 \end{aligned}$$

The Figures 9, 10 and 11 show the swell arrival time for each of the three typhoons. Each curve indicates the arrival time of energy from a source at a specified leaving time labeled with various periods (from 7 to 19 sec.).

Appendix C shows the arrival time calculations for each typhoon.

Figure 9 Typhoon Hope

Swell arrival time

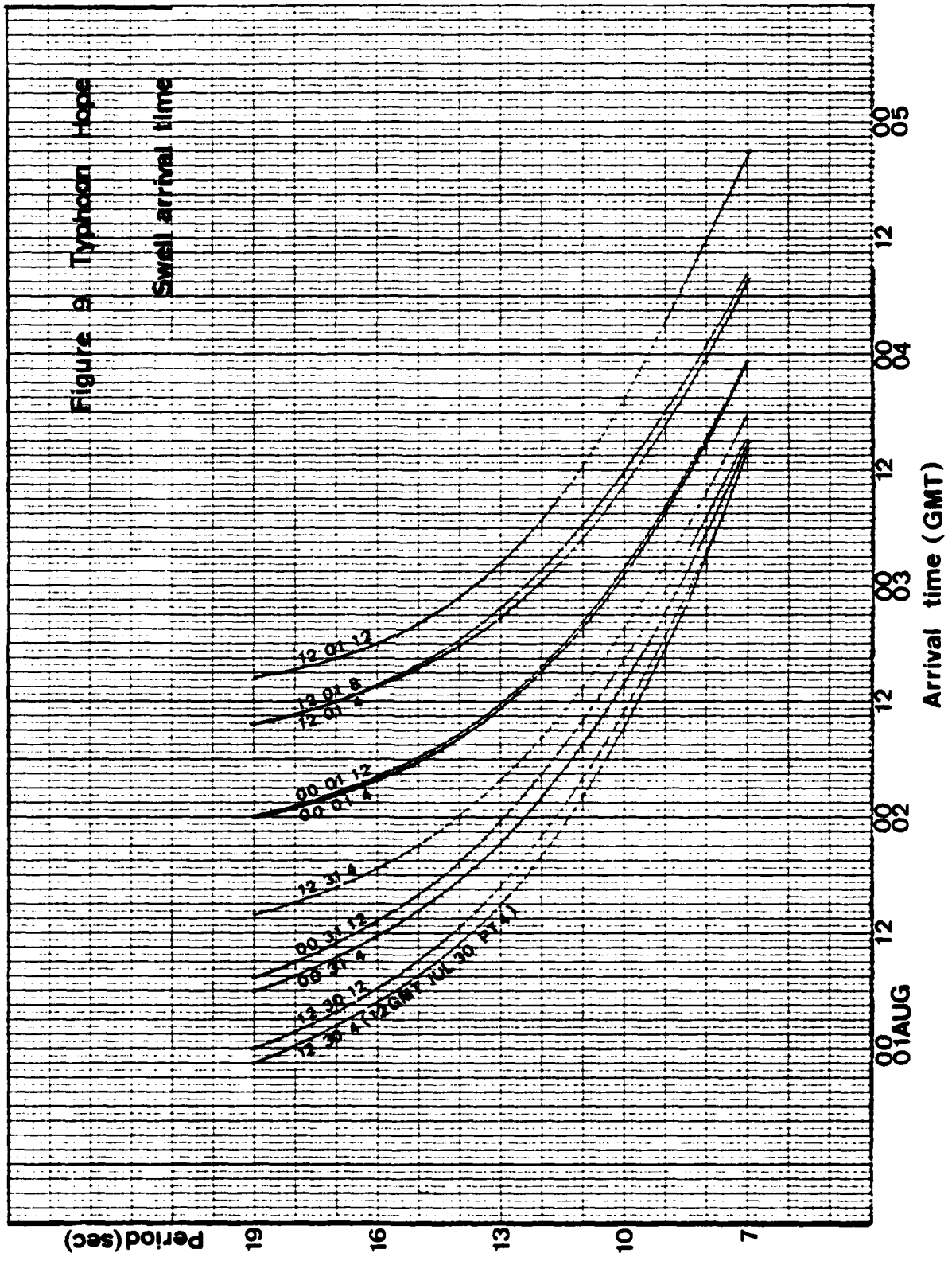


Figure 10 Typhoon Irving

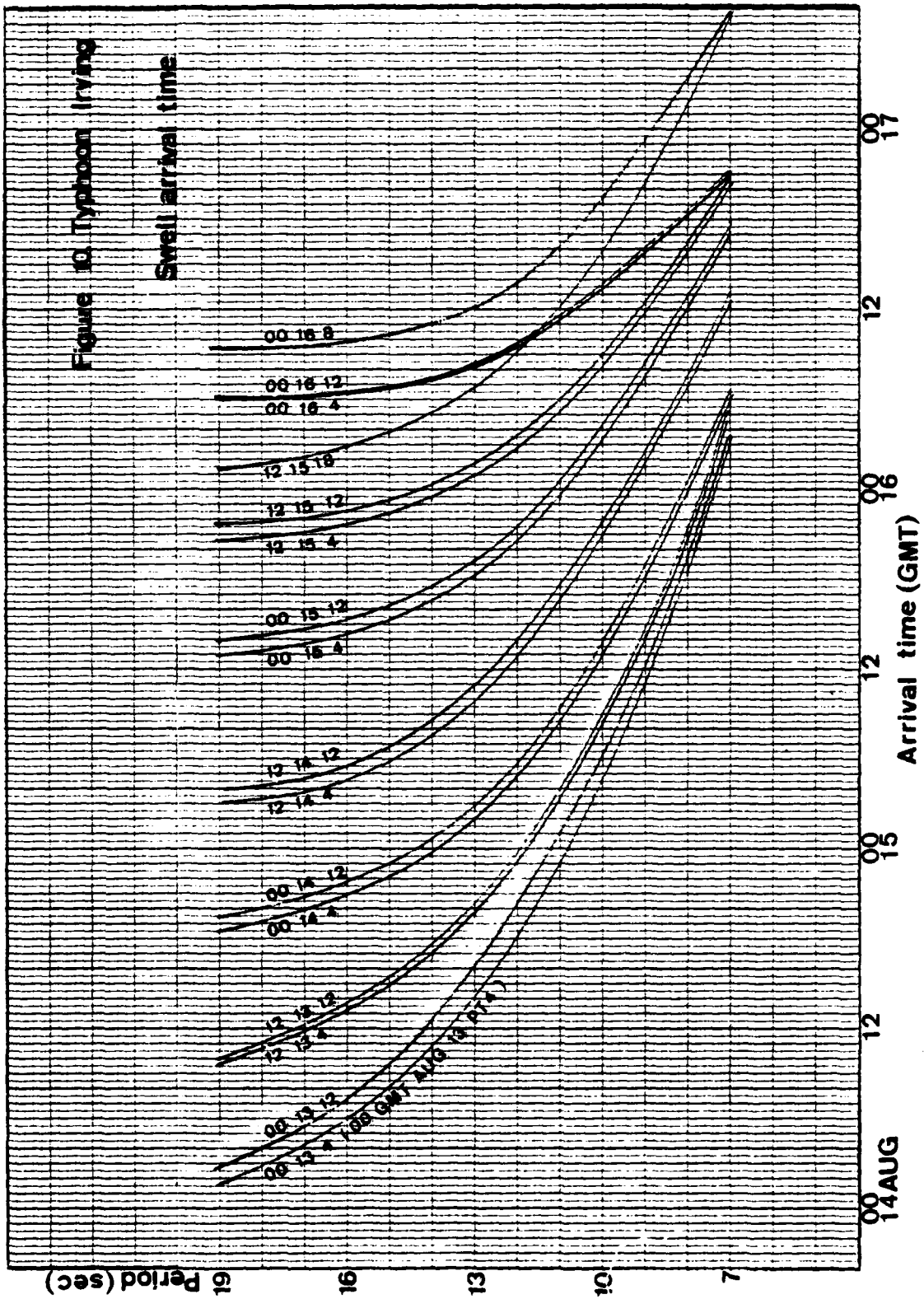
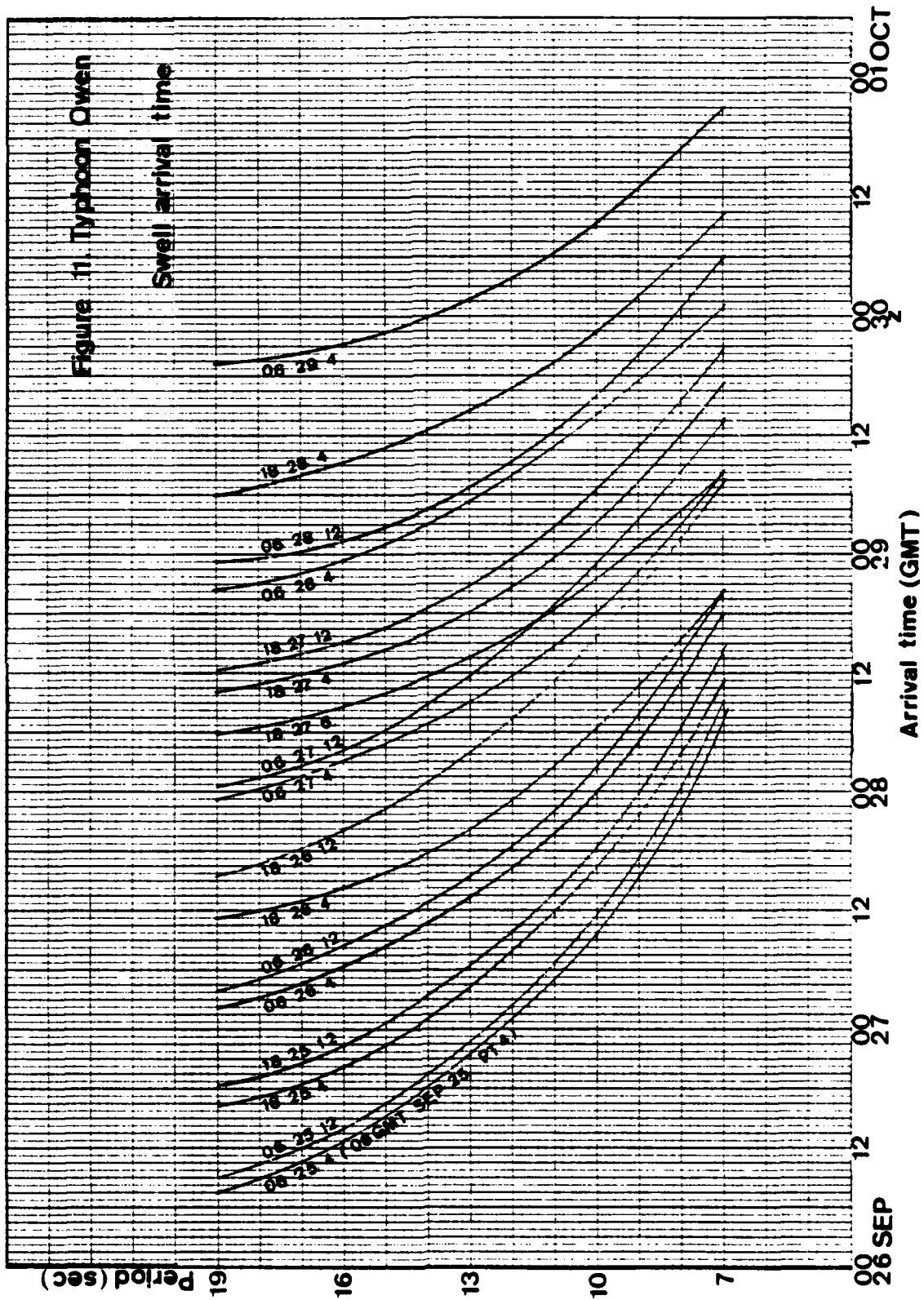


Figure 11 Typhoon Owen



IV. THE ENERGY PROPAGATION PROCEDURE

A. PROPAGATION OF SPECTRAL ENERGY COMPONENTS

The spectral forecast permits the forecaster to deal with only that range of periods which have important energy. Each spectral component is tracked with its respective group velocity, only those directions being chosen for which waves can reach Cheju-do. When the typhoon is moving with a velocity component toward Cheju-do, only spectral components with a group velocity greater than the movement of the typhoon are considered (as in Typhoon Irving).

Wave energy generated in a relatively small region at all frequencies will spread over a much larger region as it propagates outward from its source, and the wave characteristics change in such a way as to become more "swell like." There are essentially three processes which contribute to this change in wave characteristics: dispersion and angular spreading, which are modified by shoaling and refraction, and attenuation.

In the procedure followed here, I have ignored attenuation for waves of long period. Dispersion and angular spreading are accounted for by simply following components to Cheju-do with appropriate shoaling and refraction factors.

For ease of calculation shoaling and refraction processes are simplified as described below. As seen on Map 1, a slightly curved contour of 100 fathoms (590 ft) connects the northern tip of Taiwan to the south-western tip of Japan. The slope from 590 ft bottom line to 413 ft (70 fathoms) is very steep. But most bottom topography along the path to Cheju-do, north of the 413 ft bottom contour is almost flat with the depth of 45 fathoms (266 ft) up to the forecast site ($33.2^{\circ}\text{N } 126.6^{\circ}\text{E}$).

Therefore, I have approximated to underwater topography by assuming only two water depths, a deep water and a shallow water (intermediate water depth) region with an abrupt jump between them.

To compute the wave characteristics at a shoal water site, the shoaling and refraction are considered using the values of C_g and n from Chapter III.B.

The energy of component $E_0(\bar{T}, \bar{\theta})$ in the typhoon area (deep water) is transformed after shoaling and refraction to its value at the forecast site according to

$$E(i, j) = E_0(i, j) \cdot k_s^2(i, j) k_r^2(i, j)$$

where $E(i, j)$ is the energy of the component of period \bar{T}_i and which had the direction θ_j in the generating area,

and $k_s(i, j)$, $k_r(i, j)$ are the respective shoaling and refraction factors of those components.

Details of calculation of k_s and k_r are given in the following sections. The refraction and shoaling calculations for three typhoons are shown in Appendix D. The following is a sample calculation on 12 GMT July 30 for Typhoon Hope at source point 4.

\bar{T}	7	10	13	16	19
k_s	1	1	0.92	0.89	0.90
k_r	1	1	1	0.989	0.972
$(k_s k_r)^2$	1	1	0.8464	0.7748	0.7653
E_o	7	19	11	9	14
E	7	19	9.3	7.0	10.7

where k_s is derived from plate C-1 [6]

with $h = 40$ fathoms = 236 ft

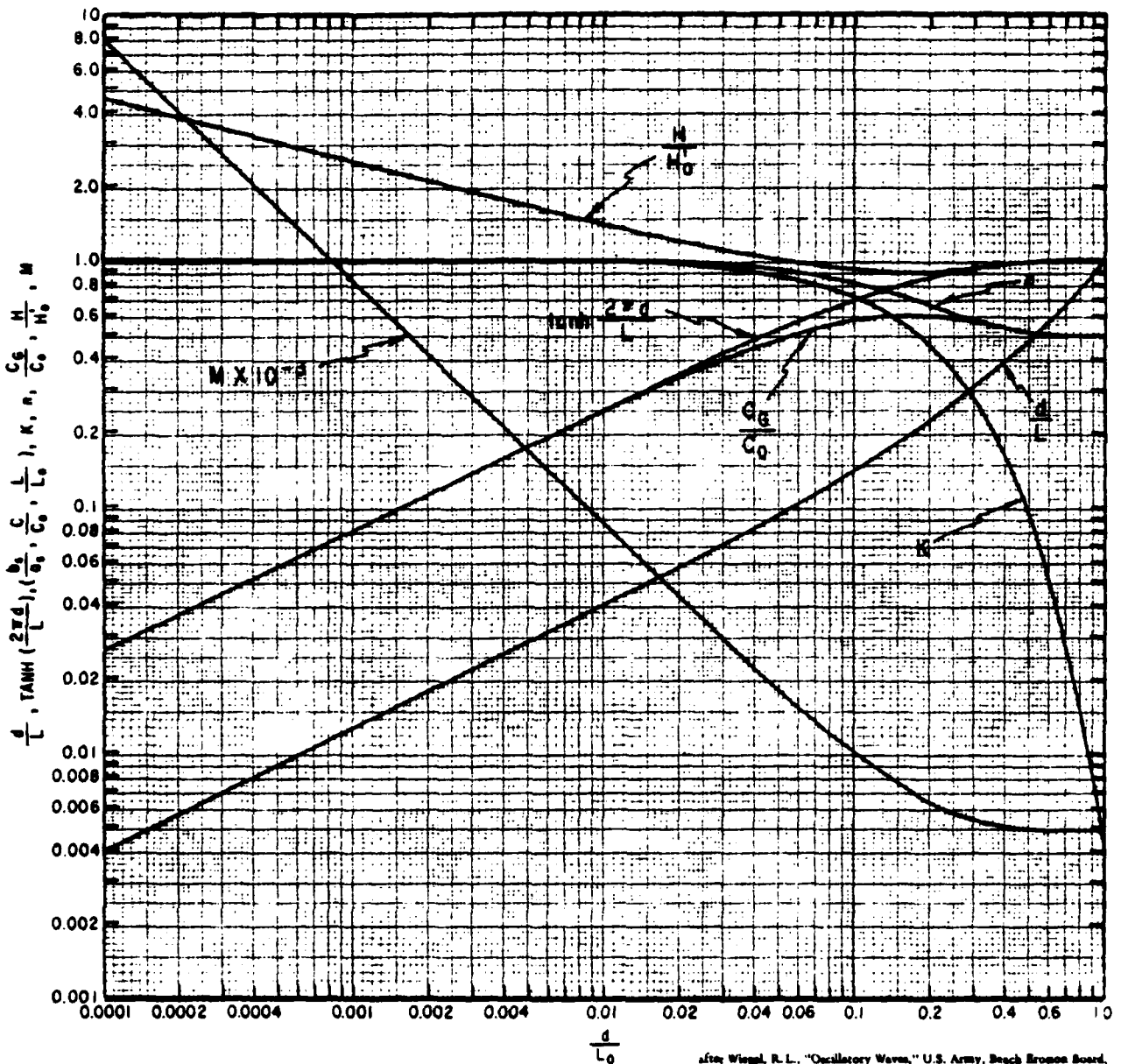
k_r is derived from Figure 2-19 [5]

with $h = 413$ ft and $\alpha_o = 40^\circ$.

B. SHOALING AND REFRACTION FACTOR

1. Shoaling Factor

The shoaling factor, $k_s = H/H'_o$ was derived from the plate C-1 [6] with depth and period of the appropriate spectral component. The shoal site depth near Cheju-do ($33.2^\circ\text{N } 126.6^\circ\text{E}$) is 40 fathoms, and the relative depth h/L_o and shoaling factor of each period are shown below.



after Weigl, R. L., "Oscillatory Waves," U.S. Army, Beach Erosion Board, Bulletin, Special Issue No. 1, July 1948.

Plate C-1. Illustration of Various Functions of $\frac{d}{L_0}$

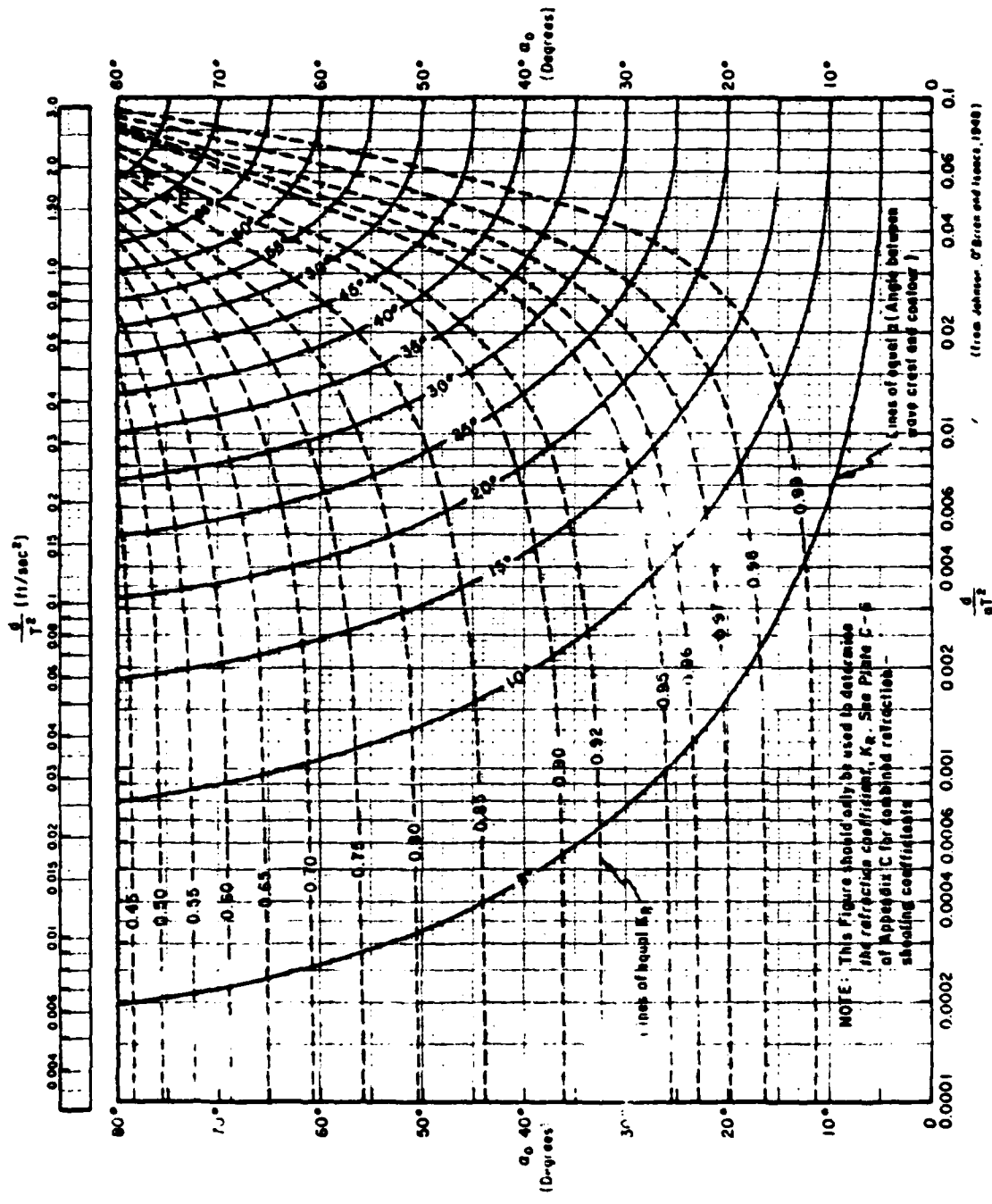


Figure 2-19 Changes in Wave Direction and Height Due to Refraction on Slopes with Straight, Parallel Depth Contours

\bar{T}	17	10	13	16	19
h/L_0	0.94	0.46	0.24	0.18	0.13
k_s	1	1	0.92	0.89	0.90

2. Refraction Factor

Generally, two basic techniques of refraction analysis are available--graphical and numerical. Several graphical procedures are available, but all methods of refraction analyses are based upon Snell's law. Refraction may be treated analytically in any region with straight and parallel contours, by using Snell's law directly: $\sin \alpha = \left(\frac{c}{c_0}\right) \sin \alpha_0$, where α is the angle between the wave crest and the bottom contour, and α_0 is the angle between the deep water wave crest and the bottom contour.

Figure 2-19 [5] shows the relationships among α , α_0 , period, depth and refraction factor in graphical form. I derived the refraction factor from using this graph, Figure 2-19, the bottom contour and period. Also, I assumed that the refraction factor is 1 if the angle α_0 (between crest and bottom contour) is less than 10° and that the refraction occurs only one time at the depth of maximum bottom gradient where waves are refracted because of the wide flat-bottomed portions over most of the intermediate water propagation path as seen on Map 1.

With these considerations, I derived the refraction factor and predicted the shoaling energy. Those procedures are shown in Appendix D.

C. SHOALING AND REFRACTION OF THE SPECTRAL COMPONENTS

Each deep water wave spectral component derived from the TYWAVES model moves with its respective group velocity. I considered the 80 energy components to behave as monochromatic component waves. To assess the shoaling and refraction of each to the shoal-water site I assumed that the wave power transmitted between a given pair of orthogonals remains constant at all depths (this means no frictional losses, diffraction or scattering, and also implies that a steady state exists).

With these assumptions the wave power P is given by

$$P = E C_g b = E_o C_{g_o} b_o$$

$$\text{Thus, } E = E_o \frac{C_{g_o} b_o}{C_g b} = E_o \times k_s^2 k_r^2 = \frac{1}{8} \rho g H^2$$

where E = the average wave energy per unit area of sea surface for waves transformed by shoaling and refraction.

ρ = water density

g = acceleration of gravity

H = wave height of transformed waves

C_{g_o}, C_g = group velocity

b_o, b = orthogonal separations

k_s = shoaling factor

k_r = refraction factor

The energy in each spectral component of the swell at the observation site was calculated by modifying the energy spectrum at the selected sources for the effects of shoaling and refraction according to equation $E = E_o \cdot k_s^2 \cdot k_r^2$.

The energy associated with the various components as a function of time of arrival at observation site, as seen in Figures 9, 10 and 11.

The total energy in the swell at any given arrival time is estimated by summing all the shoaling components at that time.

In summary, each component in typhoon area's $\bar{T} - \theta$ spectrum is shoaled and refracted using the k_s and k_r values appropriate to it to find the energy at the observation site.

1. Shoaling Process (Computation)

See Appendix D.

2. Shoaling Energy Components From Each Source Versus Arrival Time

As seen in Figures 12, 14 and 16, the energy of the components from all sources is shown as a function of its arrival time at Cheju. See Appendix D.

3. The Predicted Swell Waves at Prediction Site

As shown in Figures 13, 15 and 17, the predicted swell waves are the sum of all transformed components at given time at the forecast site.

For Typhoon Irving (see Figure 15) beginning 12 GMT August 16, the forecast site is already inside typhoon area. Therefore, there is no prediction done after that time. These predictions are discussed in Chapter IV.D.

D. THE OBSERVED DATA

Observations of wave conditions for verification of the swell forecasts were obtained from the sources, the National Oceanographic Data Center (NODC) and the Republic of Korea (ROK) Navy. All listed heights are based on visual estimates.

Following Table VIII shows the visual observation of swell heights ($H_{1/10}$) for each typhoon. The data from NODC are sparse and often far from the forecast site, but they appear to be samples from the same set as those of the ROK Navy. The data from ROK Navy visual observations were made at 33.2°N , 126.5°E close to my point of interest (33.2°N , 126.6°E). So I considered this point exactly the same as my forecast site.

Figure 14 Typhoon Irving

Directional energy propagation

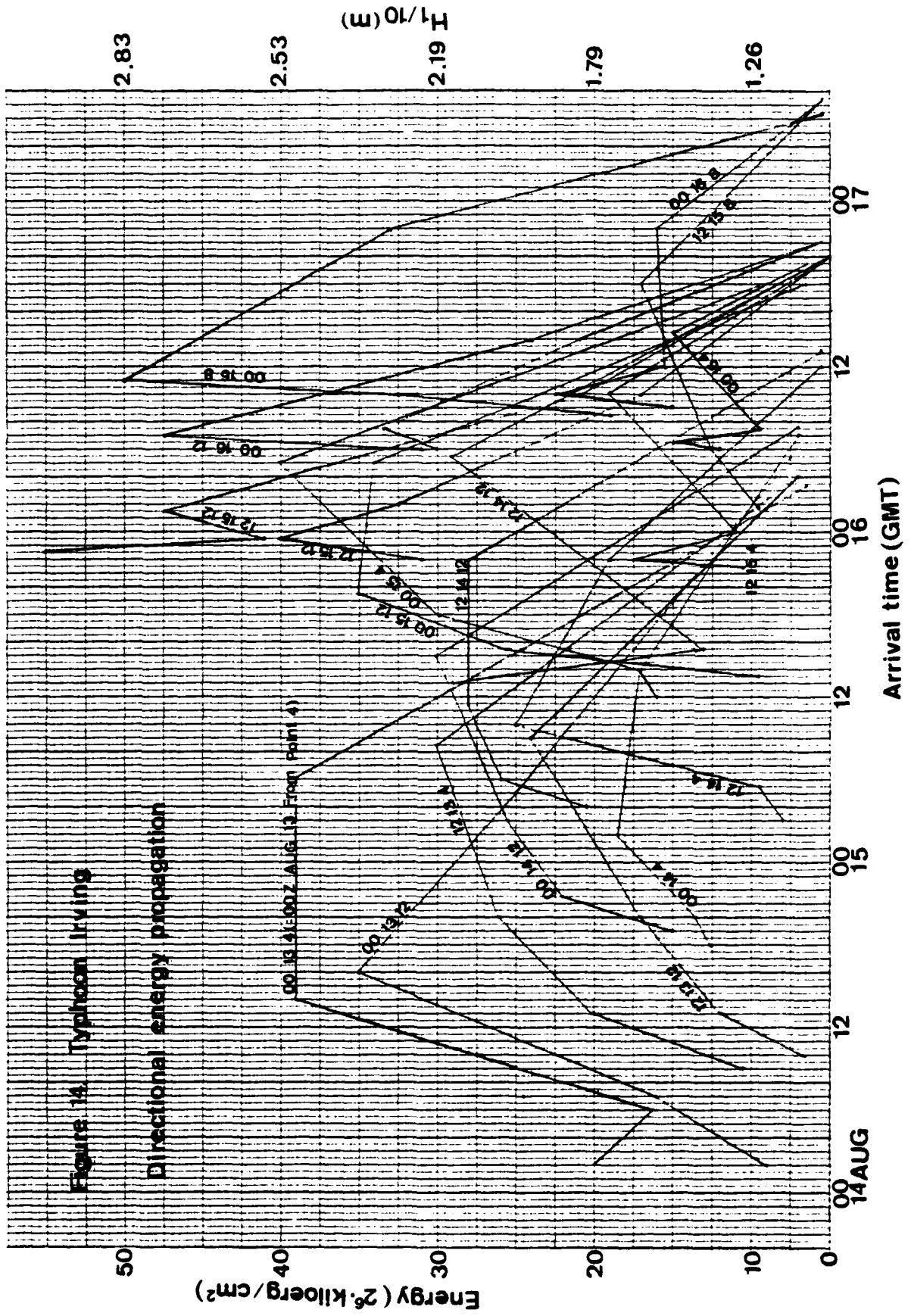


Figure 16- Typhoon Owen

Directional energy propagation

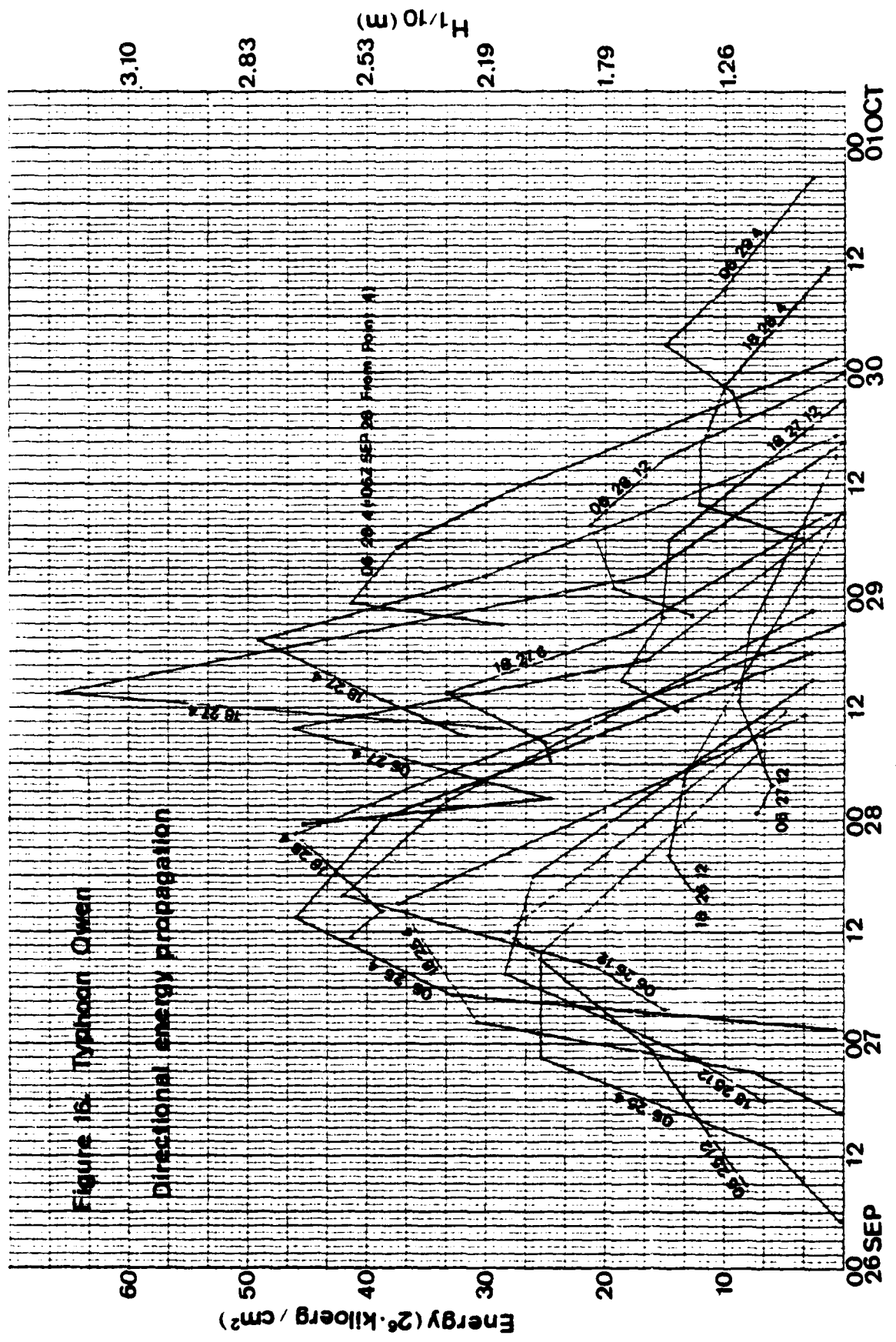
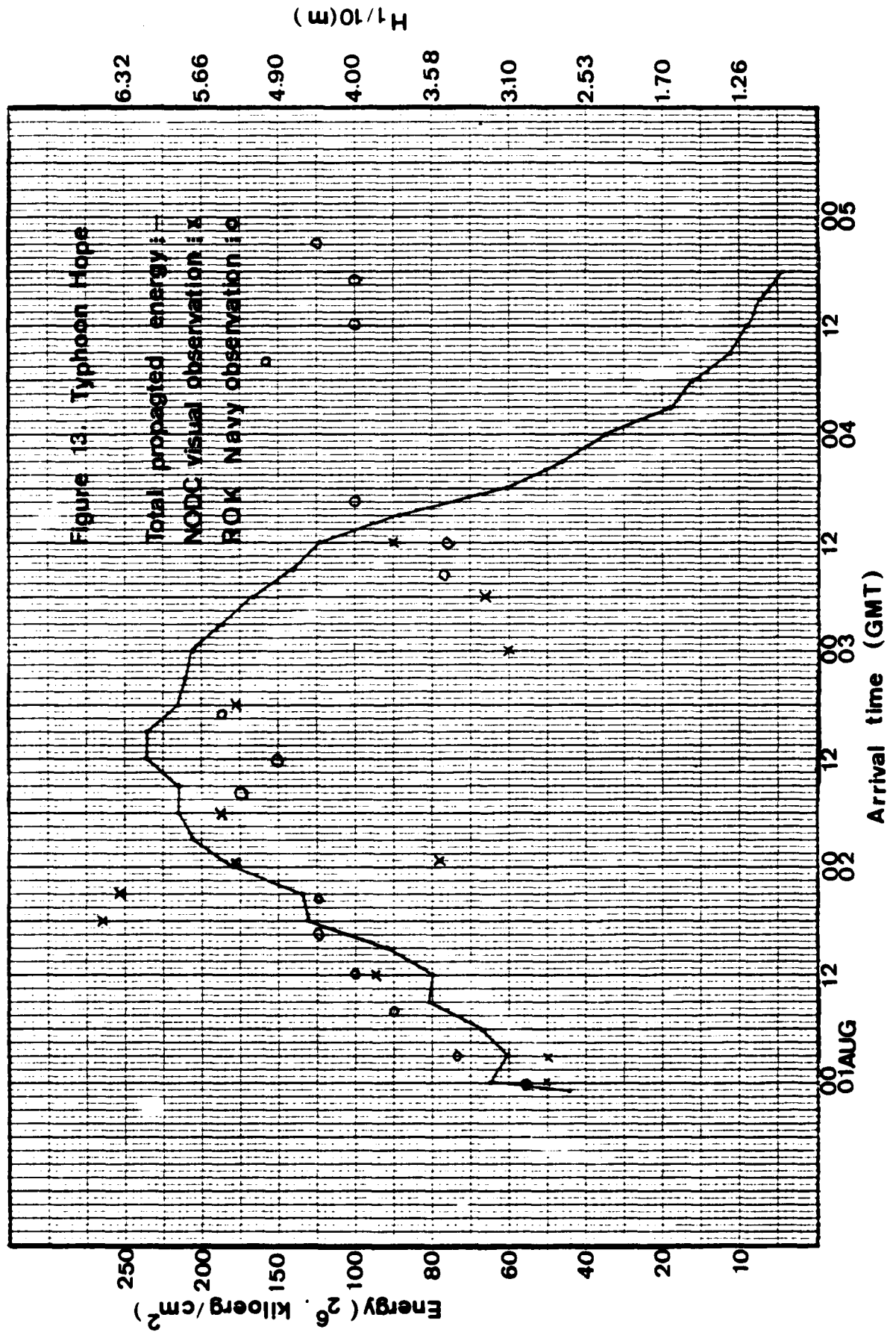


Figure 13. Typhoon Hope



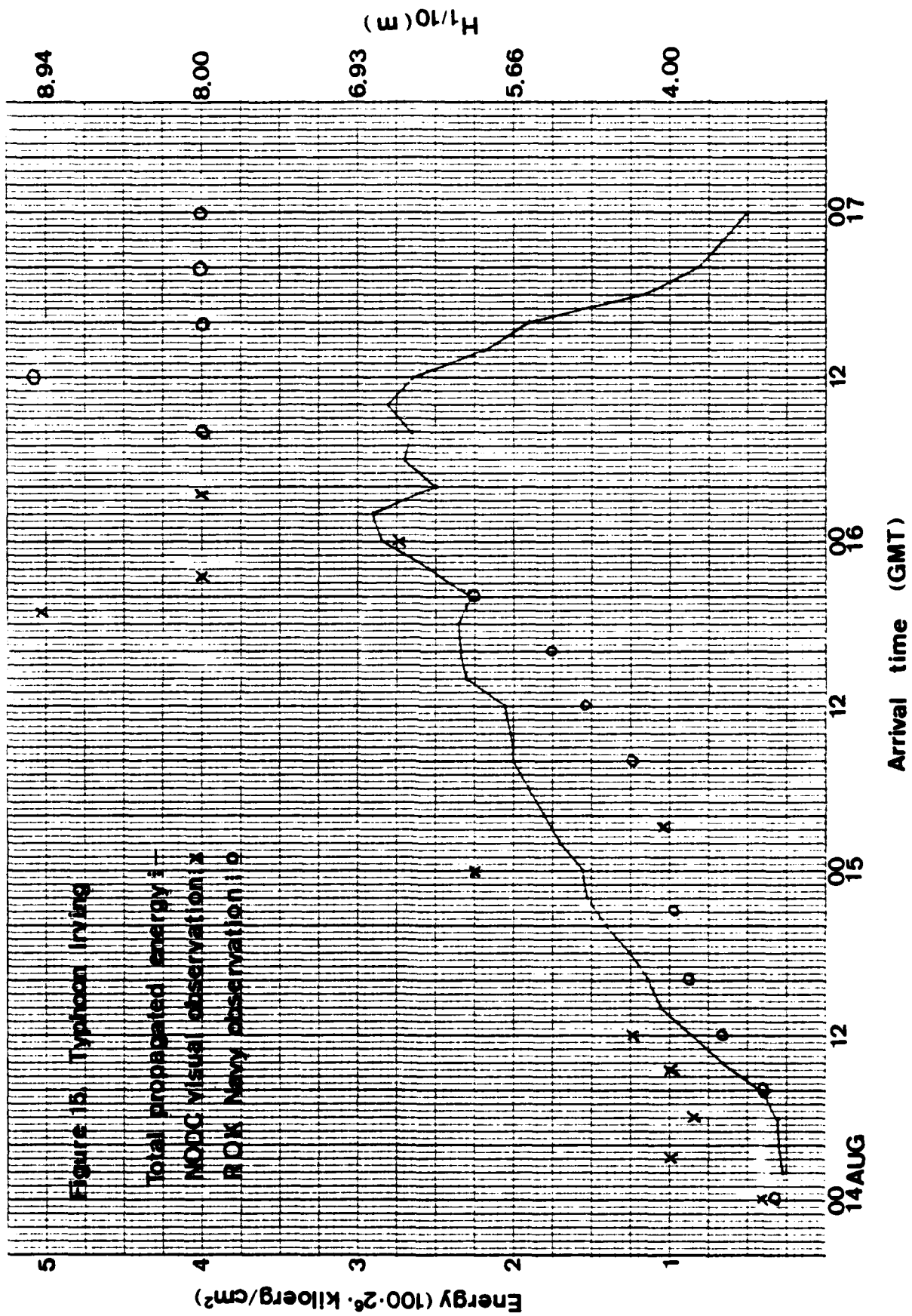


TABLE 8

The Visual Observation Data by NODC and ROK Navy

1. For Typhoon Hope

<u>DTG (GMT)</u>	<u>Location ($^{\circ}$N-$^{\circ}$E)</u>	<u>H 1/10 (meters)</u>	<u>Source</u>
79080100	33.6-125.2	2.5	NODC
0104	32.3-126.0	2.5	NODC
0112	31.2-126.7	4.0	NODC
0118	27.7-124.6	6.5	NODC
0121	27.8-125.4	6.5	NODC
0200	29.1-128.0	6.5	NODC
0206	28.0-129.0	5.5	NODC
0218	26.9-125.8	5.0	NODC
0300	28.7-128.6	3.0	NODC
0306	31.4-126.2	3.0	NODC
0312	32.3-125.9	3.5	NODC
080100	33.2-126.5	3.0	ROK Navy
0104	33.2-126.5	3.5	ROK Navy
0108	33.2-126.5	3.7	ROK Navy
0112	33.2-126.5	4.0	ROK Navy
0116	33.2-126.5	4.5	ROK Navy
0120	33.2-126.5	4.5	ROK Navy
0208	33.2-126.5	5.0	ROK Navy
0212	33.2-126.5	4.5	ROK Navy
0216	33.2-126.5	5.5	ROK Navy
0220	33.2-126.5	4.5	ROK Navy
0308	33.2-126.5	3.5	ROK Navy
0312	33.2-126.5	3.5	ROK Navy
0316	33.2-126.5	3.0	ROK Navy
0320	33.2-126.5	5.0	ROK Navy
0408	33.2-126.5	4.0	ROK Navy
0412	33.2-126.5	3.0	ROK Navy
0416	33.2-126.5	3.0	ROK Navy
0420	33.2-126.5	2.5	ROK Navy

2. For Typhoon Irving

<u>DTG (GMT)</u>	<u>Location (°N-°E)</u>	<u>H 1/10 (meters)</u>	<u>Source</u>
79081400	29.10127.6	2.5	NODC
1403	28.5-127.6	4.0	NODC
1406	28.7-129.3	3.5	NODC
1409	27.7-129.7	4.0	NODC
1412	29.2-131.1	4.5	NODC
1500	30.0-125.0	6.0	NODC
1503	30.7-127.3	4.0	NODC
1515	28.3-130.3	8.0	NODC
1518	27.2-130.0	9.0	NODC
1521	26.5-128.8	8.0	NODC
1600	27.1-130.0	6.5	NODC
1603	27.3-128.5	8.0	NODC
1606	29.6-129.2	5.5	NODC
1700	27.4-125.5	6.0	NODC
79081400	33.2-126.5	2.5	ROK Navy
1408	33.2-126.5	2.5	ROK Navy
1412	33.2-126.5	3.0	ROK Navy
1416	33.2-126.5	3.5	ROK Navy
1420	33.2-126.5	3.5	ROK Navy
1508	33.2-126.5	4.0	ROK Navy
1512	33.2-126.5	4.5	ROK Navy
1516	33.2-126.5	5.0	ROK Navy
1520	33.2-126.5	6.0	ROK Navy
1608	33.2-126.5	8.0	ROK Navy
1612	33.2-126.5	9.0	ROK Navy
1616	33.2-126.5	8.0	ROK Navy
1620	33.2-126.5	8.0	ROK Navy
1708	33.2-126.5	8.0	ROK Navy
1712	33.2-126.5	9.0	ROK Navy
1716	33.2-126.5	8.0	ROK Navy
1720	33.2-126.5	7.0	ROK Navy

3. For Typhoon Owen

<u>DTG (GMT)</u>	<u>Location (°N-°E)</u>	<u>H 1/10 (meters)</u>	<u>Source</u>
79092600	31.4-128.0	4.0	NODC
2606	33.6-129.1	3.5	NODC
2615	31.8-129.5	3.0	NODC
2700	28.1-126.9	6.0	NODC
2703	27.1-126.6	6.5	NODC
2706	32.6-125.7	4.0	NODC
2709	31.6-125.7	5.5	NODC
2712	30.7-129.8	6.5	NODC
2715	28.7-125.3	6.0	NODC
2800	32.8-128.3	5.5	NODC
2803	30.6-125.7	6.5	NODC
2806	31.5-126.8	6.5	NODC
2809	31.6-126.6	6.0	NODC
2812	31.7-126.6	6.5	NODC
2818	34.0-128.3	6.0	NODC
2900	32.7-127.7	6.5	NODC
2606	32.1-127.3	5.5	NODC
2912	31.0-126.4	5.5	NODC
2918	34.0-129.7	5.0	NODC
3000	29.0-124.7	4.0	NODC
3006	30.8-127.7	3.0	NODC
3018	30.4-131.6	4.0	NODC
79092600	33.2-126.5	2.5	ROK Navy
2608	33.2-126.5	4.0	ROK Navy
2612	33.2-126.5	5.0	ROK Navy
2616	33.2-126.5	5.0	ROK Navy
2620	33.2-126.5	4.5	ROK Navy
2708	33.2-126.5	4.5	ROK Navy
2712	33.2-126.5	5.5	ROK Navy
2716	33.2-126.5	5.0	ROK Navy
2720	33.2-126.5	5.0	ROK Navy
2808	33.2-126.5	4.5	ROK Navy
2812	33.2-126.5	5.0	ROK Navy
2816	33.2-126.5	5.5	ROK Navy
2820	33.2-126.5	5.5	ROK Navy
2908	33.2-126.5	4.5	ROK Navy
2912	33.2-126.5	4.5	ROK Navy
2916	33.2-126.5	4.0	ROK Navy
2920	33.2-126.5	4.5	ROK Navy
3008	33.2-126.5	5.0	ROK Navy
3012	33.2-126.5	4.0	ROK Navy
3016	33.2-126.5	2.5	ROK Navy
3020	33.2-126.5	3.0	ROK Navy

E. COMPARISON OF SWELL PREDICTIONS AND OBSERVATIONS

The predicted and observed heights are plotted in Figures 13, 15 and 17, and are in good agreement. Detailed comparisons for each typhoon follow:

1. Typhoon Hope

The first predicted swell arrival times from each of three sources, and the NODC and ROK Navy observations are almost the same with similar energies (see Figure 13).

The peak energy arrival times are also nearly the same, but the peak predicted energy is slightly higher than the observations. This is reasonable agreement since it is estimated that the visual observations can be in error. Verploegh [18] estimated the average observational error for a visual observation of wave height varies from 1 ft at 5 ft wave heights to 3 ft at 18 ft wave heights.

2. Typhoon Irving

As seen in Figure 15, the predicted swell arrival time nearly matches the time shown by both sets of observations. However, the predicted energy of the rise is slightly higher than the observational values. The peak energy (around the time of 20 GMT August 15) is also the same as the observational peak.

After 00 GMT August 16, the prediction site is within the typhoon's wind circulation area. Most wave heights ($H_{1/10}$) are 8m and the highest observation is 10m. These waves

dominate the entire wave field and no swell can be distinguished later than 00 GMT August 16.

3. Typhoon Owen

In Typhoon Owen (see Figure 17), the swell arrival time indicated by observations is earlier than the predicted time by about 6-12 hours. The predicted peak energy lies close to the observational values.

In fact, the NODC values are higher than those of the prediction, and ROK Navy observations are lower. Except near the peak both observation sets show similar time variations. Therefore, the observed values are considered consistent and probably accurate.

F. ERROR SOURCES

I have made several assumptions in this study in order to simplify calculations. The most serious error sources involve assumptions about the windows in the Ryukyu Islands, group velocity in shallow water, and simple bottom contours in shallow water.

There are also differences between the predictions (which include waves dependent on the local weather conditions) that make it difficult to evaluate the prediction. Regarding the assumptions about group velocity in Chapter III.B, I used $n = 3/4$ in shallow water for calculation of group velocity $C_g = nc$. In Typhoon Hope, which has the longest shallow water travel distance, miscalculation of C_g would have its

greatest effect. Yet the observed and predicted energy peaks are not greatly separated. This may mean that the approximations are realistic.

The bottom contour assumptions seem to be reasonable through three tests. The local weather condition is the most serious factor contributing to differences between the observations and the predictions. The local wind pattern was the following at Cheju-do, according to the ROK Navy data set.

1979	072900-073100:	SW 5-8 kts (preceding Hope swell)
	080100-080300:	SW 6-10 kts (during Hope swell)
1979	081200-081300:	S 6-8 kts (preceding Irving swell)
	081400-081700:	S 30-60 kts (during Irving swell)
	092400-092600:	E 5-8 kts (preceding Owen swell)
	092600-093000:	E 20-30 kts (during Owen swell)

Therefore, before the swell arrivals, the local wave heights were considered less than 1-1.5 m. During Irving and Owen there were important local sea contributions to observed height.

Lastly, the original error sources, i.e., those involving input parameters for the TYWAVES model, the location of the typhoon center, the winds in the source region, and typhoon

size, etc., are ignored in this study. Those errors are discussed in Refs. [2] and [17].

V. CONCLUSIONS

From Figures 13, 15 and 17, I can conclude that most predicted swell heights are lower than those of the observations (combined sea and swell).

The times of occurrence of the predicted peak heights agreed reasonably well with those of observations for the swell from each typhoon.

These results on the basis of this limited test suggest that TYWAVES predict satisfactorily those swells in the East China Sea which originate in tropical cyclones in the western North Pacific.

Computer aided predictions may improve the quality of the forecasts by reducing the need for simplifying approximations, as in the case of the treatment in this thesis of the shoaling and refraction processes. Such predictions would also provide a larger base for assessing the accuracy of the method. Additional verification is required to draw more specific conclusions.

APPENDIX A

Outputs of TYWAVES For Typhoon Owen at 12 GMT September 26

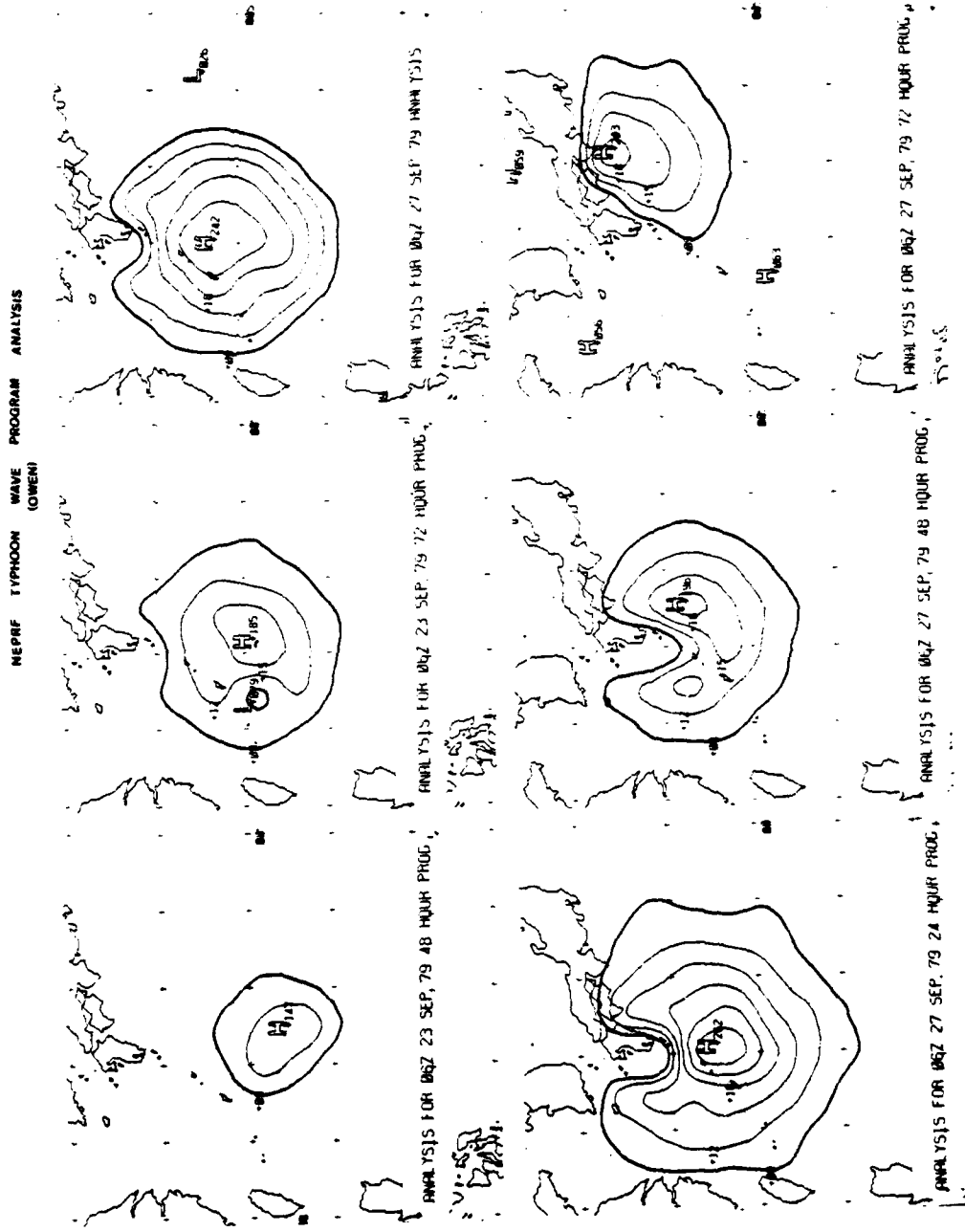
The following tables and figures show the computer analysis for Typhoon Owen by TYWAVES.

- a. Period-directional spectrum at each of 12 sources.
- b-1. The significant wave height ($H_{1/3}$ in feet) distribution in typhoon area. "0" indicates the land area and the distance between the grid points is 40 NM.
- b-2. The maximum wave period distribution in typhoon area. "-1" indicates the land area.
- b-3. The maximum wind wave directions distribution.
The direction indicated with 16 unit point rose, from North (1) to NNE (16) with CCW direction.
- c. NEPRF Typhoon Wave Program Analysis for Typhoon Owen during the typhoon period from the time of the first typhoon warning to 72 hours later, based on post-analysis data.

TYPHOON WAVES		POINT 7		TYPHOON WAVES		POINT 8		TYPHOON WAVES		POINT 9	
M.I./I = 5.9 M		AZIMUTH 36		M.I./I = 7.1 M		AZIMUTH 36		M.I./I = 5.1 M		AZIMUTH 36	
NORTH CORRESPONDS TO THE		NORTH CORRESPONDS TO THE		NORTH CORRESPONDS TO THE		NORTH CORRESPONDS TO THE		NORTH CORRESPONDS TO THE		NORTH CORRESPONDS TO THE	
N	1	0	0	0	0	0	0	0	0	0	0
NNE	0	0	0	0	0	0	0	0	0	0	0
NE	0	0	0	0	0	0	0	0	0	0	0
NNE	0	0	0	0	0	0	0	0	0	0	0
ENE	0	0	0	0	0	0	0	0	0	0	0
E	0	0	0	0	0	0	0	0	0	0	0
ESE	0	0	0	0	0	0	0	0	0	0	0
E	0	0	0	0	0	0	0	0	0	0	0
ESE	0	0	0	0	0	0	0	0	0	0	0
SE	0	0	0	0	0	0	0	0	0	0	0
SSE	0	0	0	0	0	0	0	0	0	0	0
S	0	0	0	0	0	0	0	0	0	0	0
SSW	0	0	0	0	0	0	0	0	0	0	0
SW	0	0	0	0	0	0	0	0	0	0	0
WSW	0	0	0	0	0	0	0	0	0	0	0
W	0	0	0	0	0	0	0	0	0	0	0
WNW	0	0	0	0	0	0	0	0	0	0	0
NW	12	3	31	40	29	14					
NNW	37	3	17	7	9	1					
TOTAL	211	0	16	75	57	56	17				
PERIODS	4	7	1	13	16	19					

TYPHOON WAVES		POINT 11		TYPHOON WAVES		POINT 12	
M.I./I = 6.5 M		AZIMUTH 36		M.I./I = 5.2 M		AZIMUTH 36	
NORTH CORRESPONDS TO THE		NORTH CORRESPONDS TO THE		NORTH CORRESPONDS TO THE		NORTH CORRESPONDS TO THE	
N	0	0	0	0	0	0	0
NNE	0	0	0	0	0	0	0
NE	0	0	0	0	0	0	0
NNE	0	0	0	0	0	0	0
ENE	0	0	0	0	0	0	0
E	0	0	0	0	0	0	0
ESE	0	0	0	0	0	0	0
E	0	0	0	0	0	0	0
ESE	0	0	0	0	0	0	0
SE	0	0	0	0	0	0	0
SSE	0	0	0	0	0	0	0
S	0	0	0	0	0	0	0
SSW	0	0	0	0	0	0	0
SW	0	0	0	0	0	0	0
WSW	0	0	0	0	0	0	0
W	0	0	0	0	0	0	0
WNW	0	0	0	0	0	0	0
NW	158	0	2	37	46	38	
NNW	54	0	2	11	25	8	
NW	4	0	6	2	6	0	
NNW	0	0	1	0	0	0	
TOTAL	272	0	9	63	94	52	51
PERIODS	4	7	1	13	16	19	

c. NEPRF Typhoon Wave Program Analysis for Typhoon Owen during the typhoon period from the time of the first typhoon warning to 72 hours later, based on post-analysis data.





ANALYSIS FOR 06Z 27 SEP 79 12 HOUR PROG.

[Handwritten signature]

APPENDIX B

Sea Spectra at Source Region for Three Typhoons and Significant Wave Distribution

The following tables and figures show the period-direction spectrum at selected source grid point and NEPRF typhoon wave program analysis for wave height ($H_{1/3}$ in feet) distribution around the typhoon center, respectively.

- a-1. NEPRF Typhoon Wave Model (period-direction spectrum at each selected grid point) for Typhoon Hope.
- a-2. NEPRF Typhoon Wave Program Analysis for Typhoon Hope.
- b-1. NEPRF Typhoon Wave Model (period-direction spectrum at each selected source grid point) for Typhoon Irving.
- b-2. NEPRF Typhoon Wave Program Analysis for Typhoon Irving.
- c-1. NEPRF Typhoon Wave Model (period-direction spectrum at each selected source grid point) for Typhoon Owen.
- c-2. NEPRF Typhoon Wave Program Analysis for Typhoon Owen.

a-1. NEPRF Typhoon Wave Model
(Hope)

NEPRF TYPHOON WAVE MODEL
(HOPE)

1979 07 30 12		TYPHOON WAVES		POINT 4		TYPHOON		POINT 12		TYPHOON WAVES		POINT 4	
NORTH CORRESPONDS TO THE		M.1/10= 6.2 M		AZIMUTH 360		07 30 12		M.1/10= 7.8 M		AZIMUTH 360		07 31 00	
M		0		0		0		0		0		M	
MNE	0	0	0	0	0	0	0	0	0	0	0	0	0
ME	0	0	0	0	0	0	0	0	0	0	0	0	0
ENE	0	0	0	0	0	0	0	0	0	0	0	0	0
E	13	0	0	12	0	0	0	0	0	0	0	0	0
ESE	55	0	0	30	15	0	0	0	0	0	0	0	0
SE	105	0	0	39	46	0	15	0	0	0	0	0	0
SSE	63	0	0	7	19	11	9	14	0	0	0	0	0
S	0	0	0	0	0	0	0	0	0	0	0	0	0
SSW	2	0	0	0	0	0	0	0	0	0	0	0	0
SM	0	0	0	0	0	0	0	0	0	0	0	0	0
MSM	0	0	0	0	0	0	0	0	0	0	0	0	0
M	0	0	0	0	0	0	0	0	0	0	0	0	0
MNW	0	0	0	0	0	0	0	0	0	0	0	0	0
MM	0	0	0	0	0	0	0	0	0	0	0	0	0
MNW	0	0	0	0	0	0	0	0	0	0	0	0	0
TOTAL	245	0	21	103	81	9	30	0	106	0	18	77	84
TOTAL PERIODS	4	7	10	13	16	19			4	7	10	13	16

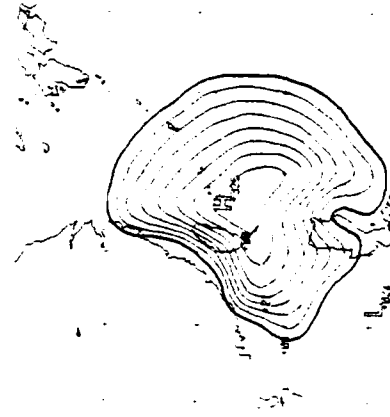
07 31 00		TYPHOON WAVES		POINT 4		TYPHOON		POINT 12		TYPHOON WAVES		POINT 4	
NORTH CORRESPONDS TO THE		M.1/10= 12.3 M		AZIMUTH 360		08 01 00		M.1/10= 14.5 M		AZIMUTH 360		08 01 00	
M		0		0		0		0		0		M	
MNE	0	0	0	0	0	0	0	0	0	0	0	0	0
ME	0	0	0	0	0	0	0	0	0	0	0	0	0
ENE	0	0	0	0	0	0	0	0	0	0	0	0	0
E	0	0	0	0	0	0	0	0	0	0	0	0	0
ESE	2	0	0	1	0	0	0	0	0	0	0	0	0
SE	72	0	0	27	23	19	19	0	100	0	3	56	9
SSE	123	0	0	3	37	43	19	19	121	0	0	14	0
S	67	0	0	2	17	19	16	11	44	0	0	3	0
SSW	0	0	0	0	0	0	0	0	49	0	0	11	18
SM	0	0	0	0	0	0	0	0	0	0	0	0	0
MSM	0	0	0	0	0	0	0	0	0	0	0	0	0
M	0	0	0	0	0	0	0	0	0	0	0	0	0
MNW	0	0	0	0	0	0	0	0	0	0	0	0	0
MM	0	0	0	0	0	0	0	0	0	0	0	0	0
MNW	0	0	0	0	0	0	0	0	0	0	0	0	0
TOTAL	266	0	10	82	89	44	89	0	457	0	9	47	132
TOTAL PERIODS	4	7	10	13	16	19			4	7	10	13	16

TYPHOON		POINT 12	TYPHOON		POINT 11	TYPHOON		POINT 9
CORRESPONDS TO THE		AZIMUTH 16	CORRESPONDS TO THE		AZIMUTH 16	CORRESPONDS TO THE		AZIMUTH 16
08 0100		M. 1/1 = 12.0 M	08 0112		M. 1/1 = 11.0 M	08 0112		M. 1/1 = 1.0 M
N	1	1	N	5	1	N	1	1
NNE	1	1	NNE	5	1	NNE	1	1
NF	1	1	NF	5	1	NF	1	1
ENE	1	1	ENE	5	1	ENE	1	1
E	1	1	E	5	1	E	1	1
ESE	1	1	ESE	5	1	ESE	1	1
SSE	1	1	SSE	5	1	SSE	1	1
S	1	1	S	5	1	S	1	1
SSW	1	1	SSW	5	1	SSW	1	1
SW	1	1	SW	5	1	SW	1	1
WSW	1	1	WSW	5	1	WSW	1	1
W	1	1	W	5	1	W	1	1
WNW	1	1	WNW	5	1	WNW	1	1
WN	1	1	WN	5	1	WN	1	1
NNW	1	1	NNW	5	1	NNW	1	1
N	1	1	N	5	1	N	1	1
TOTAL 926		7 14 15 16 19	TOTAL 769		6 9 13 14 16 19	TOTAL 661		3 11 12 13 14 15

TYPHOON		POINT 12	TYPHOON		POINT 12
CORRESPONDS TO THE		AZIMUTH 16	CORRESPONDS TO THE		AZIMUTH 16
08 0112		M. 1/1 = 11.0 M	08 0112		M. 1/1 = 11.0 M
N	1	1	N	1	1
NNE	1	1	NNE	1	1
NF	1	1	NF	1	1
ENE	1	1	ENE	1	1
E	1	1	E	1	1
ESE	1	1	ESE	1	1
SSE	1	1	SSE	1	1
S	1	1	S	1	1
SSW	1	1	SSW	1	1
SW	1	1	SW	1	1
WSW	1	1	WSW	1	1
W	1	1	W	1	1
WNW	1	1	WNW	1	1
WN	1	1	WN	1	1
NNW	1	1	NNW	1	1
N	1	1	N	1	1
TOTAL 782		1 2 9 22 26 196	TOTAL 782		1 2 9 22 26 196

a-2. NEPRF Typhoon Wave Program Analysis
(Hope)

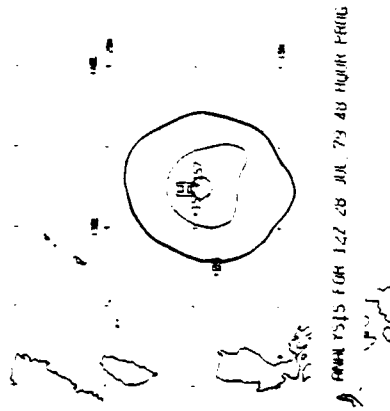
NEPRF TYPHOON WAVE PROGRAM ANALYSIS
(HOPE)



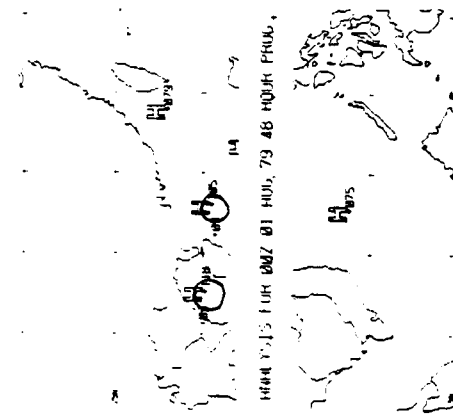
01 HOU, 79 HNE T.T.S.



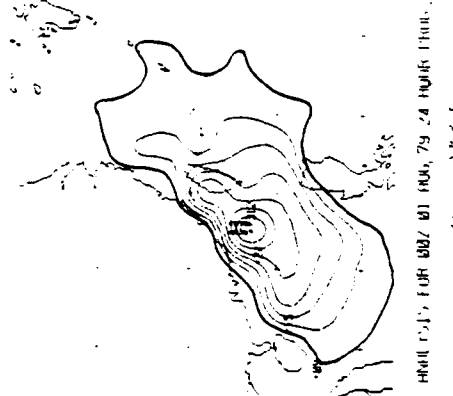
28 JUL, 79 72 HOUR PROG.



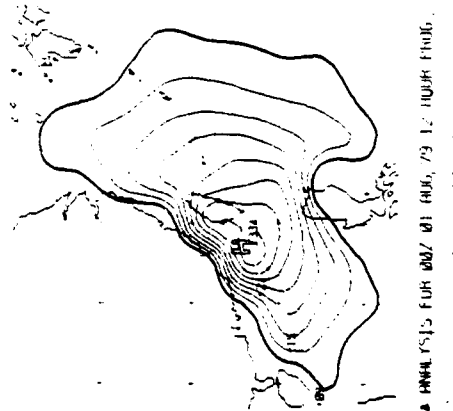
28 JUL, 79 48 HOUR PROG.



01 HOU, 79 48 HOUR PROG.



01 HOU, 79 24 HOUR PROG.



01 HOU, 79 12 HOUR PROG.

b-1. NEPRF Typhoon Wave Model
(Irving)

NEPRF TYPHOON WAVE MODEL
(IRVING)

1979 081300		POINT 12		POINT 4		POINT 1	
M.171 = 5.0 M		M.171 = 5.0 M		M.171 = 6.0 M		M.171 = 6.0 M	
NORTH CORRESPONDS TO THE		AZIMUTH 16		NORTH CORRESPONDS TO THE		AZIMUTH 16	
N	1	0	0	0	0	0	0
NNE	1	0	0	0	0	0	0
NE	1	0	0	0	0	0	0
NNE	1	0	0	0	0	0	0
ENE	1	0	0	0	0	0	0
E	1	0	0	0	0	0	0
ESE	1	0	0	0	0	0	0
SE	25	1	1	1	1	1	1
SSE	17	1	1	1	1	1	1
S	43	1	1	1	1	1	1
SSW	7	1	1	1	1	1	1
SW	1	1	1	1	1	1	1
WSW	1	1	1	1	1	1	1
W	1	1	1	1	1	1	1
WNW	1	1	1	1	1	1	1
W	1	1	1	1	1	1	1
WNW	1	1	1	1	1	1	1
WNW	1	1	1	1	1	1	1
TOTAL	222	16	64	76	34	27	
PERIODS		4	7	11	13	16	19

1979 081312		POINT 12		POINT 4		POINT 1	
M.171 = 5.0 M		M.171 = 5.0 M		M.171 = 6.0 M		M.171 = 6.0 M	
NORTH CORRESPONDS TO THE		AZIMUTH 16		NORTH CORRESPONDS TO THE		AZIMUTH 16	
N	1	0	0	0	0	0	0
NNE	1	0	0	0	0	0	0
NE	1	0	0	0	0	0	0
NNE	1	0	0	0	0	0	0
ENE	1	0	0	0	0	0	0
E	1	0	0	0	0	0	0
ESE	2	0	0	0	0	0	0
SE	24	1	1	1	1	1	1
SSE	17	1	1	1	1	1	1
S	43	1	1	1	1	1	1
SSW	7	1	1	1	1	1	1
SW	1	1	1	1	1	1	1
WSW	1	1	1	1	1	1	1
W	1	1	1	1	1	1	1
WNW	1	1	1	1	1	1	1
W	1	1	1	1	1	1	1
WNW	1	1	1	1	1	1	1
WNW	1	1	1	1	1	1	1
TOTAL	171	9	37	39	41	37	
PERIODS		4	7	11	13	16	19

TYPHOON WAVES	POINT 1	TYPHOON WAVES	POINT 1
081412 M.171 = 7.5 M		081412 M.171 = 5.5 M	
NORTH CORRESPONDS TO THE AZIMUTH 56		NORTH CORRESPONDS TO THE AZIMUTH 56	
N	1	N	1
NNE	0	NNE	0
NW	0	NW	0
ENE	1	ENE	1
E	1	E	1
ESE	1	ESE	1
SE	2	SE	1
SSE	16	SSE	1
S	19	S	1
SSW	1	SSW	1
SW	1	SW	1
WSW	1	WSW	1
W	1	W	1
WNW	1	WNW	1
NW	1	NW	1
NNW	1	NNW	1
TOTAL	39	TOTAL	23
PERIODS	4 7 1 13 16 19	PERIODS	4 7 13 15 19

TYPHOON WAVES	POINT 12	TYPHOON WAVES	POINT 12
081500 M.171 = 6.4 M		081512 M.171 = 4.9 M	
NORTH CORRESPONDS TO THE AZIMUTH 56		NORTH CORRESPONDS TO THE AZIMUTH 56	
N	1	N	1
NNE	1	NNE	1
NW	0	NW	0
ENE	0	ENE	0
E	0	E	0
ESE	1	ESE	1
SE	2	SE	1
SSE	11	SSE	1
S	15	S	1
SSW	1	SSW	1
SW	1	SW	1
WSW	1	WSW	1
W	1	W	1
WNW	1	WNW	1
NW	1	NW	1
NNW	1	NNW	1
TOTAL	39	TOTAL	23
PERIODS	4 7 1 13 16 19	PERIODS	4 7 13 15 19

(IRVING)

TYPHOON WAVES		POINT 8	
M.1/11 = 9.8 M		M.1/11 = 9.8 M	
NORTH CORRESPONDS TO THE AZIMUTH 360			
N	0	0	0
NNE	0	0	0
NE	0	0	0
NNE	0	0	0
ENE	0	0	0
E	0	0	0
ESE	0	0	0
SE	3	0	0
SSE	13	0	0
S	62	0	0
SSW	164	0	0
SM	197	0	0
MSM	101	0	0
M	52	0	0
MNW	3	0	0
NW	1	0	0
NNW	0	0	0
TOTAL	600	0	0
PERIODS	4	7	10

TYPHOON WAVES		POINT 7	
M.1/11 = 7.9 M		M.1/11 = 7.9 M	
NORTH CORRESPONDS TO THE AZIMUTH 360			
N	0	0	0
NNE	0	0	0
NE	0	0	0
ENE	0	0	0
E	0	0	0
ESE	25	0	0
SE	135	0	0
SSE	164	0	0
S	65	0	0
SSW	0	0	0
SM	0	0	0
MSM	0	0	0
M	0	0	0
MNW	0	0	0
NW	0	0	0
NNW	0	0	0
TOTAL	390	0	0
PERIODS	4	7	13

TYPHOON WAVES		POINT 6	
M.1/11 = 8.0 M		M.1/11 = 8.0 M	
NORTH CORRESPONDS TO THE AZIMUTH 360			
N	0	0	0
NNE	0	0	0
NE	0	0	0
ENE	0	0	0
E	0	0	0
ESE	0	0	0
SE	0	0	0
SSE	0	0	0
S	91	0	0
SSM	175	0	0
SM	119	0	0
MSM	16	0	0
M	0	0	0
MNW	0	0	0
NW	0	0	0
NNW	0	0	0
TOTAL	492	0	0
PERIODS	4	7	10

TYPHOON WAVES		POINT 12	
M.1/11 = 7.7 M		M.1/11 = 7.7 M	
NORTH CORRESPONDS TO THE AZIMUTH 360			
N	0	0	0
NNE	0	0	0
NE	0	0	0
ENE	0	0	0
E	0	0	0
ESE	2	0	0
SE	172	0	0
SSE	179	0	0
S	122	0	0
SSW	2	0	0
SM	0	0	0
MSM	0	0	0
M	0	0	0
MNW	0	0	0
NW	0	0	0
NNW	0	0	0
TOTAL	379	0	0
PERIODS	4	7	10

b-2. NEPRF Typhoon Wave Program Analysis
(Irving)

NEPRF TYPHOON WAVE PROGRAM ANALYSIS
(IRVING)



ANALYSIS FOR 00Z 13 AUG 79 HRR 1515
ANALYSIS FOR 00Z 13 AUG 79 12 HOUR PROG
ANALYSIS FOR 00Z 13 AUG 79 24 HOUR PROG

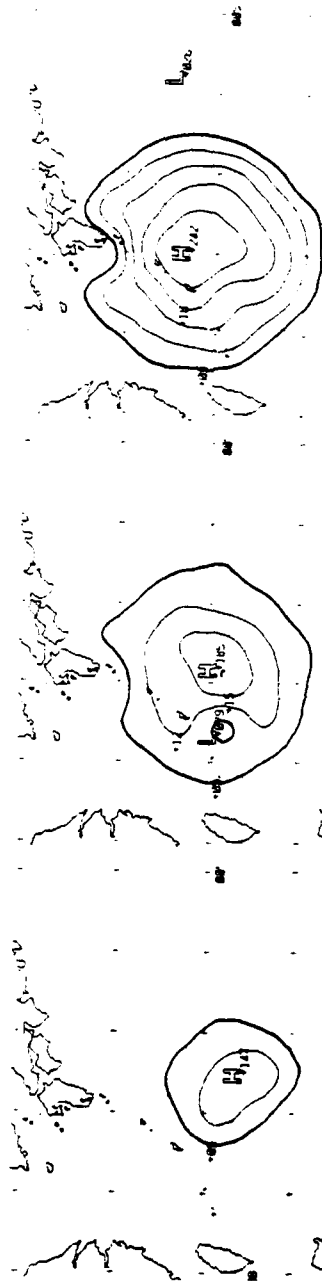
ANALYSIS FOR 00Z 13 AUG 79 48 HOUR PROG
ANALYSIS FOR 00Z 13 AUG 79 72 HOUR PROG

TYPHOON WAVES	POINT 4	TYPHOON WAVES	POINT 12	TYPHOON WAVES	POINT 5
092618		092618		092706	
M.1/1 = 10.1		M.1/1 = 4.5		M.1/1 = 4.0	
AZIMUTH 51		AZIMUTH 360		AZIMUTH 76	
N	0	0	0	0	0
NE	0	0	0	0	0
E	0	0	0	0	0
SE	19	0	0	0	0
S	142	0	0	0	0
SW	192	0	0	0	0
WSW	15	0	0	0	0
W	0	0	0	0	0
WNW	0	0	0	0	0
NW	0	0	0	0	0
NNW	0	0	0	0	0
TOTAL	645	0	0	0	0
PERIODS	4	7	10	13	16

TYPHOON WAVES	POINT 4	TYPHOON WAVES	POINT 12	TYPHOON WAVES	POINT 5
092708		092718		092718	
M.1/1 = 4.0		M.1/1 = 4.7		M.1/1 = 7.4	
AZIMUTH 76		AZIMUTH 15		AZIMUTH 76	
N	0	0	0	0	0
NE	0	0	0	0	0
E	0	0	0	0	0
SE	37	0	0	0	0
S	140	0	0	0	0
SW	122	0	0	0	0
WSW	42	0	0	0	0
W	0	0	0	0	0
WNW	0	0	0	0	0
NW	0	0	0	0	0
NNW	0	0	0	0	0
TOTAL	424	0	0	0	0
PERIODS	4	7	10	13	16

C-2. NEPRF Typhoon Wave Program Analysis
(Owen)

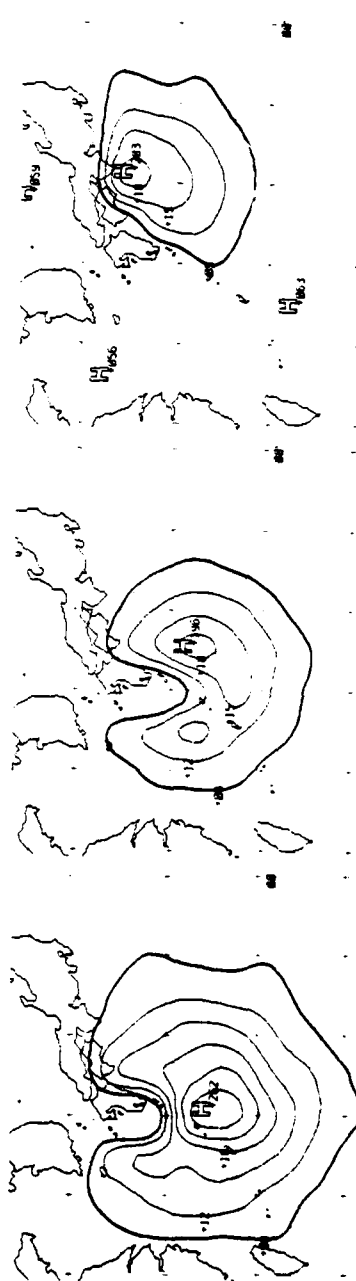
NEPRF TYPHOON WAVE PROGRAM ANALYSIS
(OWEN)



ANALYSIS FOR 06Z 23 SEP 79 48 HOUR PROG.

ANALYSIS FOR 04Z 23 SEP 79 72 HOUR PROG.

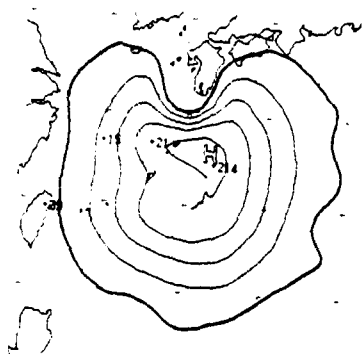
ANALYSIS FOR 04Z 27 SEP 79 84 HOURS



ANALYSIS FOR 06Z 27 SEP 79 24 HOUR PROG.

ANALYSIS FOR 06Z 27 SEP 79 48 HOUR PROG.

ANALYSIS FOR 06Z 27 SEP 79 72 HOUR PROG.



ANALYSIS FOR 06Z 27 SEP. 79 12 HOUR PROG.

APPENDIX C

Propagation Energy Arrival Time

The following tables show the components from each source grid point, travel time and arrival time (GMT).

R_0 and R are determined from Map 1 (U.S. Navigation Chart No. 94027, Scale 1: 927.700 at lat $32^{\circ}15'$) from the critical depth of each period.

			Cgo/Cgs	10.6	15.2	18.7/29.4	24.3/33.6	28.8/35.8
			T	7	10	13	16	19
12 Jul 30 (GMT)	PT4 17.4-133.9	Ro/R	1036	1036	896/140	873/163	866/170	
		t	97.74	68.16	52.67	40.78	34.82	
		tar	031344	0202809	011640	010447	312249	
	PT12 17.4-135.3	Ro/R	1071	1071	941/130	876/175	884/187	
		t	101.03	70.46	54.74	42.08	35.91	
		tar	031702	021028	011844	010605	312355	
00 Jul 31	PT4 18.6-131.5	Ro/R	919	919	749/170	719/200	709/210	
		t	86.70	60.46	45.83	34.94	30.49	
		tar	031443	021228	012150	011056	010629	
	PT12 18.6-132.9	Ro/R	946	946	816/130	781/165	770/176	
		t	89.29	62.24	48.06	37.05	31.66	
		tar	031717	021414	020004	011303	010740	
12 Jul 31	PT4 19.6-128.3	Ro/R	822	822	610/212	555/267	550/272	
		t	77.55	54.08	39.83	30.79	26.70	
		tar	031731	021847	020350	011847	011442	
00 Aug 01	PT4 20.6-125.3	Ro/R	780	780	410/370	370/440	365/415	
		t	73.56	51.32	34.52	27.43	24.26	
		tar	040134	030319	021031	020326	020014	
	PT12 20.6-126.8	Ro/R	756	756	501/255	476/280	471/285	
		t	71.32	49.74	35.46	27.92	24.31	
		tar	032319	030144	021128	020355	020019	
12 Aug 01	PT4 21.5-122.2	Ro/R	744	744	324/420	284/460	279/465	
		t	70.19	48.95	31.62	25.38	22.68	
		tar	041011	031257	021937	021323	021041	
	PT8 19.5-122.2	Ro/R	858	858	446/412	408/450	406/452	
		t	80.94	56.45	37.86	30.18	26.73	
		tar	042059	032027	030152	021811	021444	
12 Aug 01	PT12 21.5-123.7	Ro/R	720	720	350/370	305/415	300/420	
		t	67.92	47.37	31.30	24.90	22.15	
		tar	040755	031122	021918	021254	021009	
00 Aug 13	PT4 20.0-128.8	Cgo/Cgs	10.6/-	15.2/-	18.7/29.4	24.3/33.6	28.8/35.8	
		Ro/R	802/-	802/-	562/240	550/252	546/256	
		t	75.66	6.76	38.22	30.13	26.11	
	PT12 20.0-130.2	Ro/R	817/-	817/-	617/200	607/210	600/217	
		t	77.08	53.75	39.80	31.23	26.89	
		tar	160505	150545	141548	140714	140253	

12 Aug 13	PT4 22.0-138.2	Ro/R	678/-	678/-	433/245	423/255	413/265
		t	63.96	44.61	31.49	25.00	21.74
		tar	160358	150837	141929	141300	140945
	PT12 22.0-129.6	Ro/R	692/-	692/-	467/225	452/240	442/250
		t	65.28	45.53	32.63	25.74	22.33
		tar	160519	150932	142038	141345	141020
00 Aug 14	PT4 23.5-127.2	Ro/R	583/-	583/-	323/260	303/280	300/283
		t	55.00	38.36	26.12	20.80	18.32
		tar	160700	151422	150207	142048	141819
	PT12 23.5-128.6	Ro/R	592/-	592/-	362/230	352/240	350/242
		t	55.85	38.95	27.18	21.63	18.91
		tar	160751	151457	150311	142138	141855
12 Aug 14	PT4 24.6-126.7	Ro/R	516/-	516/-	239/277	196/320	191/325
		t	48.68	33.95	22.20	17.59	15.71
		tar	161241	152157	151012	150535	150343
12 Aug 14	PT12 24.6-128.2	Ro/R	523/-	523/-	288/235	278/245	263/260
		t	49.34	34.41	23.39	18.73	16.39
		tar	161320	152224	151123	150614	150424
00 Aug 15	PT4 25.9-126.5	Ro/R	438/-	438/-	155/293	108/330	103/335
		t	41.32	28.82	18.25	14.27	12.93
		tar	161719	160449	151815	151416	151256
00 Aug 15	PT12 25.9-128.0	Ro/R	444/-	444/-	214/230	204/240	199/245
		t	41.89	29.10	19.27	15.53	13.75
		tar	161753	160513	151916	151532	151345
12 Aug 15	PT4 27.5-126.0	Ro/R	343/-	343/-	13/330	-/343	-/343
		t	32.36	22.57	11.92	10.21	9.58
		tar	162022	161034	152355	152213	152135
	PT8 25.5-125.9	Ro/R	464/-	464/-	144/320	119/345	109/355
		t	43.73	30.53	18.58	15.16	13.70
		tar	170744	161832	160635	160310	160142
	PT12 27.5-127.5	Ro/R	345/-	345/-	105/240	95/250	85/260
		t	32.54	22.70	13.78	11.35	10.21
		tar	162033	161042	160147	152321	152213
00 Aug 16	PT4 29.6-126.0	Ro/R	218/-	218/-	-/218	-/218	-/218
		t	20.57	14.34	7.41	6.49	6.09
		tar	162034	161421	160725	160629	160605
	PT8 27.6-126.	Ro/R	337/-	337/-	20/317	-/317	-/317
		t	31.79	22.17	11.85	10.03	9.41
		tar	170747	162210	161151	161002	160925

	PT12	Ro/R	221/-	221/-	-/221	-/221	-/221
	29.6-127.5	t	20.85	14.54	7.52	6.58	6.17
		tar	162051	161432	160731	160635	160610
06 Sep 25	PT4	Cgo/Cgs	10.6	15.2	18.0/29.4	24.3/33.6	28.8/35.8
	21.3-132.4	Ro/R	784	784	654/730	621/163	611/173
		t	73.96	51.58	39.39	30.44	26.05
		tar	280758	270935	262123	261225	260803
	PT12	Ro/R	822	822	702/120	662/160	658/164
	21.3-133.9	t	77.55	54.08	41.62	32.00	27.43
		tar	281133	271205	262337	261400	260926
18 Sep 25	PT4	Ro/R	696	696	563/133	513/183	508/188
	22.6-131.7	t	65.66	45.73	74.63	26.56	22.89
		tar	281140	271547	270438	262034	261653
	PT12	Ro/R	731	731	610/121	577/154	574/157
	22.6-133.1	t	68.96	48.09	36.74	28.32	24.32
		tar	281458	271805	270644	262219	261819
06 Sep 26	PT4	Ro/R	639	639	509/130	469/170	419/220
	23.5-131.4	t	60.28	42.04	31.64	24.36	20.07
		tar	281817	280002	271338	270622	270204
	PT12	Ro/R	675	675	555/120	522/153	515/160
	23.5-132.8	t	63.68	44.41	33.76	26.03	22.35
		tar	282141	280225	271546	270802	270421
18 Sep 26	PT4	Ro/R	542	542	417/125	382/160	371/171
	24.4-131.6	t	51.13	35.66	26.55	20.48	17.66
		tar	282108	280539	272034	271429	271140
	PT12	Ro/R	667	667	607/60	562/.05	562/105
	24.4-135.3	t	62.92	43.88	34.5	26.26	22.44
		tar	290855	281353	280430	272016	271626
06 Sep 27	PT4	Ro/R	544	544	484/60	410/134	407/137
	25.5-131.9	t	51.32	35.79	27.92	20.86	17.96
		tar	290919	281747	280955	280252	272358
	PT12	Ro/R	591	591	526/65	446/145	443/148
	25.5-133.4	t	55.75	38.88	30.34	22.67	19.52
		tar	291345	282053	281220	280440	280131
18 Sep 27	PT4	Ro/R	496	496	430/66	348/148	345/151
	26.5-132.0	t	46.79	32.63	25.24	18.73	16.20
		tar	291648	290238	281914	281244	281012

	PT6	Ro/R	406	406	306/100	251/155	245/160
	28.5-132.1	t	38.30	26.71	19.76	14.94	13.01
		tar	290818	282043	281346	280857	280706
	PT12	Ro/R	547	547	487/60	417/130	407/140
	26.5-133.5	t	51.60	35.99	28.08	21.03	18.04
		tar	292136	290559	282205	281502	281202
06 Sep 28	PT4	Ro/R	460	460	400.60	318/142	315/145
	27.3-132.1	t	43.40	30.26	23.43	17.31	14.99
		tar	300124	291216	290526	282319	282059
	PT12	Ro/R	511	511	414/97	386/125	381/130
	27.3-133.5	t	48.21	33.62	25.44	19.61	16.86
		tar	300612	291537	290726	290136	282252
18 Sep 28	PT4	Ro/R	436	436	371/65	291/145	289/147
	27.8-132.1	t	41.13	28.68	22.05	16.29	14.14
		tar	301108	292241	291603	291017	290608
06 Sep 29	PT4	Ro/R	416	416	361/55	291/125	288/128
	28.5-132.4	t	39.25	27.37	21.18	15.70	13.58
		tar	302115	300922	300311	292142	291935

APPENDIX D

Shoaling of the Spectral Energy Components

For refraction factor computation at 00 GMT August 13 from Point 4 of Typhoon Irving, the critical water depth is 325 feet and the angle between the swell crest and the bottom contour of 325 ft depth is 40° . Thus, with h/gT^2 and the Figure 2-19 [7], the refraction factors are derived like the following:

$$\begin{array}{r} \bar{T} \text{ (sec)} = 7 \quad 10 \quad 13 \quad 16 \quad 19 \\ K_r \left(\frac{H}{H_0} \right) = 1 \quad 1 \quad 1 \quad 0.98 \quad 0.963 \end{array}$$

In the same way, the other refraction factors are shown in shoaling computation, in the following tables:

1. Shoaling Computation
 - a. Typhoon Hope
 - b. Typhoon Irving
 - c. Typhoon Owen
2. Shoaling Energy and Arrival Times
 - a. Typhoon Hope
 - b. Typhoon Irving
 - c. Typhoon Owen

1. Shoaling Computation

\bar{T}	7	10	13	16	19	E (2^6 kilo- H 1/10 (in erg/cm ²) meters)	
k_s	1	1	0.92	0.89	0.90		

a. Typhoon Hope

12 Jul 30 (GMT)	PT4 17.4-133.9	k_r $(k_s k_r)^2$	1 1	1 1	1 0.8464	0.989 0.7748	0.972 0.7653	E	H 1/10
	h = 413	SSE_o	7	19	11	9	14	63	3.17
	$\alpha_o = 40^\circ$	SSE_s	7	19	9.3	7.0	10.7	53	2.91
	PT12 17.4-135.3	k_r $(k_s k_r)^2$	1 1	1 1	1 0.8464	1 0.7921	0.98 0.7779		
	h = 413	SSE_o	8	28	31	36	42	147	4.85
	$\alpha_o = 35^\circ$	SSE_s	8	28	26.2	28.5	32.7	123.4	4.44
00 Jul 31	PT4 18.6-131.5	k_r $(k_s k_r)^2$	1 1	1 1	1 0.8464	0.984 0.7670	0.962 0.7496		
	h = 413	SSE_o	4	15	20	13	15	69	3.32
	$\alpha_o = 45^\circ$	SSE_s	4	15	16.9	10.0	11.2	57.1	3.02
	PT12 18.6-132.9	k_r $(k_s k_r)^2$	1 1	1 1	1 0.8467	1 0.7921	0.982 0.7811		
	h = 431	SSE_o	3	37	43	19	19	123	4.44
	$\alpha_o = 35$	SSE	3	37	36.4	15	14.8	106.2	4.12
12 Jul 31	PT4 19.6-128.3	K_r $(k_s k_r)^2$	1 1	1 1	1 0.8464	0.984 0.767	0.962 0.75		
	n = 413	S_o	0	23	30	46	20	121	4.40
	$\alpha_o = 45^\circ$	S_s	0	23	25.4	35.3	15	98.7	3.97
00 Aug 01	PT4 20.6-123.2	k_r $(k_s k_r)^2$	1 1	1 1	0.935 0.7399	0.875 0.6065	0.825 0.5513		
	h = 236	SSW_o	5	23	30	19	40	118	4.35
	$\alpha_o = 60^\circ$	SSW_s	5	23	22.2	11.5	22.1	83.8	3.66

AD-A096 813

NAVAL POSTGRADUATE SCHOOL MONTEREY CA F/G 8/3
TEST OF THE APPLICATION OF THE TYWAVES MODEL TO PREDICTION OF S--ETC(U)
DEC 80 H S LEE

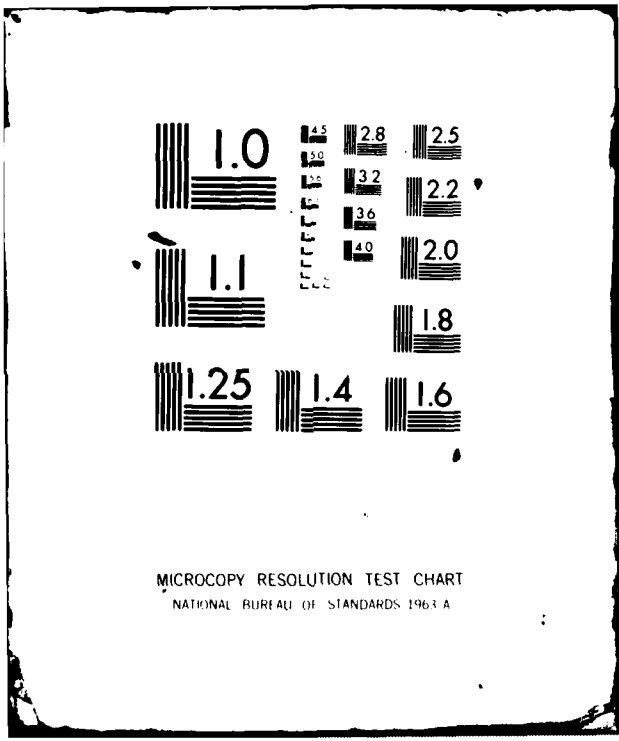
UNCLASSIFIED

NL

20
10
1



END
DATE
FILMED
F3 8
DTIC



MICROCOPY RESOLUTION TEST CHART
NATIONAL BUREAU OF STANDARDS 1963 A

	PT12	k_r	1	1	1	1	0.98		
	20.6-126.8	$(k_s k_r)^2$	1	1	0.8464	0.7921	0.7779		
	h = 413	S_o	0	20	71	98	52	243	6.24
	$\alpha_o = 35^\circ$	S_s	0	20	60.1	77.6	40.5	198.2	5.63
12 Aug 01	PT4	k_r	1	1	0.99	0.98	0.97		
	21.5-122.2	$(k_s k_r)^2$	1	1	0.8296	0.7607	0.7621		
	h = 236	SSW_o	0	11	33	3	10	58	3.05
	$\alpha_o = 30^\circ$	SSW_s	0	11	27.4	2.3	7.6	28.3	2.78
	PT8	k_r	1	1	0.97	0.93	0.88		
	19.5-122.2	$(k_s k_r)^2$	1	1	0.7963	0.6851	0.6272		
	h = 295	SSW_o	1	22	51	8	13	98	3.96
	$\alpha_o = 55^\circ$	SSW_s	1	22	40.6	5.5	8.2	77.3	3.52
	PT12	k_r	1	1	0.977	0.95	0.915		
	21.5-123.7	$(k_s k_r)^2$	1	1	0.8079	0.7149	0.6781		
	h = 295	SSW_o	0	6	17	49	31	104	4.08
	$\alpha_o = 50^\circ$	SSW_s	0	6	13.7	35.0	21	75.7	3.48

b. Typhoon Irving

00 Aug 13 (GMT)	PT4								
	20.0-128.8								
	deep	SSE	3	39	46	21	27	137	4.68m
	shoal	k_r	1	1	1	0.98	0.963		
	h = 325 ft	$(k_s k_r)^2$	1	1	0.8464	0.7607	0.7512		
	$\alpha_o = 40^\circ$	SSE	3	39	38.9	16.0	20.3	117.2	4.33

PT12

20.0-130.2

deep	SSE	5	25	38	20	11	100	4.00
shoal	k_r	1	1	1	1	1		
$h = 325$	$(k_s k_r)^2$	1	1	0.8464	0.7921	0.81		
$\alpha_o = 10$	SSE	5	25	35.0	15.8	8.9	89.7	3.79

12 Aug 13 PT4

22.0-128.2

deep	SSE	4	30	31	25	13	105	4.10
shoal	k_r	1	1	1	1	1		
$h = 325$	$(k_s k_r)^2$	1	1	0.8464	0.7921	0.81		
$\alpha_o = 10$	SSE	4	30	26.2	19.8	10.5	90.5	3.81

PT12

22.0-129.6

deep	SSE	3	24	20	15	4	67	3.27
shoal	k_r	1	1	1	1	1		
$h = 325$	$(k_s k_r)^2$	1	1	1	0.8464	0.7921	0.81	
$\alpha_o = 10$	SSE	3	24	16.9	11.9	3.2	59	3.07

00 Aug 14 PT4

23.5-125.0

deep	S	4	17	22	18	17	79	3.56
shoal	k_r	1	1	1	0.97	0.95		
$h = 325$	$(k_s k_r)^2$	1	1	0.8464	0.7453	0.7310		
$\alpha_o = 4.5$	S	4	17	18.6	13.4	12.4	65.4	3.23

PT12

23.5-128.6

deep	SSE	4	30	30	28	20	114	4.27
shoal	k_r	1	1	1	0.98	0.963		
$h = 325$	$(k_s k_r)^2$	1	1	0.8464	0.7607	0.7512		
$\alpha_o = 40$	SSE	4	30	25.4	21.3	15.0	95.7	3.91

12 Aug 14 PT4

24.6-126.7

deep	S	1	19	31	13	8	74	3.44
shoal	k_r	1	1	0.975	0.94	0.91		
$h = 266$	$(k_s k_r)^2$	1	1	0.8046	0.7	0.6708		
$\alpha_o = 50$	S	1	19	24.9	9.1	5.4	59.4	3.08

PT12

24.6-128.2

deep	SSE	1	28	33	34	27	125	4.47
shoal	k_r	1	1	1	0.98	0.963		
$h = 325$	$(k_s k_r)^2$	1	1	0.8464	0.7607	0.7512		
$\alpha_o = 40$	SSE	1	28	27.9	25.9	20.3	103.1	4.06

00 Aug 15 PT4

25.9-126.5

deep	S	9	40	36	23	22	132	4.60
shoal	k_r	1	1	0.99	0.976	0.948		
$h = 266$	$(k_s k_r)^2$	1	1	0.8296	0.7545	0.728		
$\alpha_o = 40$	S	9	40	29.9	17.4	16.0	112.3	4.24

PT12

25.9-128.0

deep	SSE_O	3	29	20	17	40	110	4.20
shoal	k_r	1	1	1	0.98	0.95		
$h = 325$	$(k_s k_r)^2$	1	1	0.8464	0.7607	0.7310		
$\alpha_O = 45$	SSE_S	3	29	16.9	12.9	29.2	91.0	3.82

"

deep	S	3	34	41	33	12	125	4.47
shoal	k_r	1	1	1	0.985	0.96		
$h = 472$	$(k_s k_r)^2$	1	1	0.8464	0.7685	0.7465		
$\alpha_O = 50$	S	3	34	34.7	25.4	9.0	106.1	4.12

12 Aug 15 PT4

27.5-126.0

deep	S	0	19	13	24	15	73	3.42
shoal	k_r	1	1	0.983	0.957	0.93		
$h = 266$	$(k_s k_r)^2$	1	1	0.8179	0.7254	0.7006		
$\alpha_O = 45$	S	0	19	10.6	17.4	10.5	57.5	3.03

PT8

25.5-125.9

deep	S	1	17	15	14	13	62	3.15
shoal	k_r	1	1	0.988	0.967	0.95		
$h = 261$	$(k_s k_r)^2$	1	1	0.8262	0.7407	0.7310		
$\alpha_O = 40$	S	1	17	12.4	10.4	9.5	50.3	2.84

PT12

29.5-127.5

deep	SSE	1	21	56	55	75	212	5.82
shoal	k_r	1	1	1	0.97	0.95		
$h = 325$	$(k_s k_r)^2$	1	1	0.8464	0.7353	0.7310		
$\alpha_o = 45$	SSE	1	1	47.4	41	54.8	145.2	4.82

PT12

27.5-127.5

deep	S	0	17	38	50	43	153	4.95
shoal	k_r	1	1	1	0.975	0.94		
$h = 384$	$(k_s k_r)^2$	1	1	0.8464	0.7530	0.7157		
$\alpha_o = 51$	S	0	17	32.2	39.9	30.8	119.9	4.38

00 Aug 16 PT4

29.6-126.0

deep	S	0	15	14	19	15	65	3.22
shoal	k_r	1	1	1	1	1		
$h = 266$	$(k_s k_r)^2$	1	1	0.8464	0.7921	0.81		
$\alpha_o = 0$	S	1	15	11.8	15.0	12.2	54	2.94

PT8

27.6-126.0

deep	S	0	16	20	31	21	90	3.79
shoal	k_r	1	1	0.983	0.957	0.93		
$h = 266$	$(k_s k_r)^2$	1	1	0.8179	0.7254	0.7006		
$\alpha_o = 45$	S	0	16	16.4	22.5	14.7	69.6	3.34

PT8

27.6-126.0

deep	SSW	0	33	62	47	31	175	5.29
shoal	k_r	1	1	0.976	0.93	0.87		
$h = 325$	$(k_s k_r)^2$	1	1	0.8063	0.6851	0.6131		
$\alpha_o = 60$	SSW	0	33	50	32.2	19	134.2	4.63

PT12

29.6-127.5

deep	SSE	1	24	54	60	38	179	5.35
shoal	k_r	1	1	1	1	1		
$h = 354$	$(k_s k_r)^2$	1	1	0.8464	0.7921	0.81		
$\alpha_o = 15$	SSE	1	24	45.7	47.5	30.8	149	4.88

PT12

29.6-127.5

deep	S	1	21	40	40	19	122	4.42
shoal	k_r	1	1	1	0.96	0.93		
$h = 384$	$(k_s k_r)^2$	1	1	0.8464	0.73	0.7001		
$\alpha_o = 50$	S	1	21	33.9	29.2	13.3	98.4	3.97

c. Typhoon Owen

06 Sep 25 (GMT)	PT4	k_r	1	1	1	1	0.98		
	21.3-132.4	$(k_s k_r)^2$	1	1	0.8464	0.7921	0.7779		
	$h = 413$ ft	$(SSE)_O$	7	26	31	8	0	74	3.44
	$\alpha_O = 35^\circ$	$(SSE)_S$	7	26	26.2	6.3	0	65.5	3.24
	PT12	k_r	1	1	1	1	0.98		
	21.3-133.9	$(k_s k_r)^2$	1	1	0.8464	0.7921	0.7779		
	$h = 413$	SSE_O	5	28	19	14	10	78	3.53
	$\alpha_O = 35$	SSE_S	5	28	16.1	11.1	7.8	68	3.30
18 Sep 25	PT4	k_r	1	1	1	0.989	0.973		
	22.6-131.7	$(k_s k_r)^2$	1	1	0.8464	0.7335	0.7716		
	$h = 413$	SSE_O	3	38	36	10	0	89	3.77
	$\alpha_O = 40$	SSE_S	3	38	30.5	7.3	0	78.8	3.55
	PT12	k_r	1	1	1	1	0.985		
	22.6-133.1	$(k_s k_r)^2$	1	1	0.8464	0.7921	0.7859		
	$h = 413$	SSE_O	2	27	34	15	9	88	3.75
	$\alpha_O = 30$	SSE_S	2	27	28.8	11.9	7.1	76.8	3.50
06 Sep 26	PT4	k_r	1	1	1	0.985	0.95		
	23.5-131.4	$(k_s k_r)^2$	1	1	0.8464	0.7685	0.73		
	$h = 384$	SSE_O	2	39	54	42	1	140	4.73
	$\alpha_O = 47$	SSE_S	2	39	45.7	32.3	0.7	119.7	4.38

	PT12	k_r	1	1	1	1	0.985		
	23.5-132.8	$(k_s k_r)^2$	1	1	0.8464	0.7921	0.7859		
	h = 384	SSE_o	2	33	49	26	19	132	4.60
	$\alpha_o = 33$	SSE_s	2	33	41.5	20.6	14.9	112	4.23
18 Sep 26	PT4	k_r	1	1	1	1	0.983		
	24.4-131.6	$(k_s k_r)^2$	1	1	0.8464	0.7921	0.0827		
	h = 384	SSE_o	0	32	54	48	53	188	5.48
	$\alpha_o = 35$	SSE_s	0	32	45.7	38	41.5	157.2	5.01
	PT12	k_r	1	1	1	1	1		
	24.4-135.3	$(k_s k_r)^2$	1	1	0.8464	0.7921	0.81		
	h = 431	SE_o	0	9	15	17	15		
	$\alpha_o < 10$	SE_s	0	9	12.7	13.5	12.2	47.4	2.75
06 Sep 27	PT4	k_r	1	1	1	1	1		
	25.5-131.9	$(k_s k_r)^2$	1	1	0.8464	0.7921	0.81		
	h = 354	SSE_o	0	17	54	31	56	150	4.90
	$\alpha_o < 10$	SSE_s	0	17	45.7	24.6	45.4	132.7	4.61
	PT12	k_r	1	1	1	1	1		
	25.5-133.4	$(k_s k_r)^2$	1	1	0.8464	0.7921	0.81		
	h = 413	SE_o	1	9	11	7	8	37	2.43
	$\alpha_o < 10$	SE_s	1	9	9.3	5.5	6.5	31.3	2.23

18 Sep 27	PT4	k_r	1	1	1	1	1		
	26.5-132.0	$(k_s k_r)^2$	1	1	0.8464	0.7921	0.81		
	h = 413	SSE_o	1	30	58	49	39	180	5.37
	$\alpha_o < 10$	SSE_s	1	30	49.1	38.8	31.6	150.5	4.91
	PT6	k_r	1	1	1	1	1		
	28.5-132.1	$(k_s k_r)^2$	1	1	0.8464	0.7921	0.81		
	h = 431	SE_o	1	18	39	32	30	123	4.44
	$\alpha_o < 10$	SE_s	1	18	33	25.3	24.3	101.6	4.03
	PT12	k_r	1	1	1	1	1		
	26.5-133.5	$(k_s k_r)^2$	1	1	0.8464	0.7921	0.81		
	h = 431	SE_o	0	15	18	23	17	75	3.46
	$\alpha_o < 10$	SE_s	0	15	15.2	18.2	13.8	62.2	3.15
	PT4	k_r	1	1	1	1	1		
	26.5-132.0	$(k_s k_r)^2$	1	1	0.8464	0.7921	0.81		
	h = 413	SE_o	0	26	57	81	35	201	5.67
	$\alpha_o < 10$	SE_s	0	26	48.2	64.2	28.4	166.8	5.17
06 Sep 28	PT4	k_r	1	1	1	1	1		
	27.3-132.1	$(k_s k_r)^2$	1	1	0.8464	0.7921	0.81		
	h = 431	SE_o	1	26	44	52	36	161	5.08
	$\alpha_o < 0$	SE_s	1	26	37.2	41.2	29.2	134.6	4.64

	PT12	k_r	1	1	1	1	1		
	27.3-133.5	$(k_s k_r)^2$	1	1	0.8464	0.7921	0.81		
	h = 431	SE_o	1	15	25	24	14	81	3.60
	$\alpha_o < 10$	SE_s	1	15	21.2	19	11.3	67.5	3.29
18 Sep 28	PT4	k_r	1	1	1	1	1		
	27.8-132.1	$(k_s k_r)^2$	1	1	0.8464	0.7921	0.81		
	h = 431	SE_o	1	10	15	16	5	49	2.80
	$\alpha_o < 10$	SE_s	1	10	12.7	12.7	4.0	40.4	2.54
06 Sep 29	PT4	k_r	1	1	1	1	1		
	28.5-132.4	$(k_s k_r)^2$	1	1	0.8464	0.7921	0.81		
	h = 431	SE_o	2	10	18	12	11	55	2.96
	$\alpha_o < 10$	SE_s	2	10	15.2	9.5	8.9	45.6	2.70

2. Shoaling Energy and Arrival Time

a. Typhoon Hope

		\bar{T}	7	10	13	16	19	SUM
12 Jul 30 (GMT)	PT4	t	97.74	68.16	52.67	40.78	34.82	
		tar	031344	020809	011640	010447	312049	
17.4-133.9		SSE_o	7	19	11	9	14	63
		SSE_s	7	19	9.3	7.0	10.7	53
	PT12	t	101.03	70.46	54.74	42.08	35.91	
		tar	031702	021028	011844	010605	312355	
17.4-135.3		SSE_o	8	28	31	36	42	147
		SSE_s	8	28	26.2	28.5	32.7	123.4

00 Jul 31	PT4	t	86.72	60.46	45.83	34.94	30.48		
		tar	031443	021228	012150	011056	010629		
	18.6-131.5	SSE _O	4	15	20	13	15	69	
		SSE _S	4	15	16.9	10.0	11.2	57.1	
		PT12	t	89.29	62.24	48.06	37.05	31.66	
			tar	031717	021414	020004	011303	010740	
18.6-132.9		SSE _O	3	37	43	19	19	123	
		SSE _S	3	37	36.4	15	14.8	106.2	
12 Jul 31		PT4	t	77.51	54.08	39.83	30.79	26.70	
			tar	031731	021847	020350	011847	011442	
	19.6-128.3	S _O	0	23	30	46	20	121	
		S _S	0	23	25.4	35.3	15	78.7	
	00 Aug 01	PT4	t	73.56	57.32	34.52	27.43	24.26	
			tar	040134	030319	021031	020326	020014	
20.6-132.2		SSW _O	5	23	30	19	40	118	
		SSW _S	5	23	22.2	115	22.1	89.8	
20.6-126.8		PT8	t	71.32	49.74	35.46	27.92	24.31	
			tar	032319	030144	021128	020355	020019	
	S _O	0	20	71	98	52	243		
		S _S	0	20	60.1	77.6	40.5	198.2	
12 Aug 01	PT4	t	70.19	48.95	31.62	25.38	22.68		
		tar	041011	031257	021937	021323	021041		
	21.5-122.2	SSW _O	0	11	33	3	10	58	
		SSW _S	0	11	27.4	2.3	7.6	48.3	

PT8	t	80.98	56.45	37.86	30.18	26.73	
	tar	042059	032027	030152	021811	021444	
19.5-122.2	SSW _O	1	22	51	81	13	98
	SSW _S	1	22	40.6	5.5	8.2	77.3
PT12	t	67.92	47.37	31.30	24.90	22.15	
	tar	040755	031122	021918	021254	021009	
21.5-123.7	SSW _O	0	6	17	49	31	104
	SSW _S	0	6	13.7	35.0	21	75.7

b. Typhoon Irving

		\bar{T}	7	10	13	16	19	SUM
00 Aug 13	PT4	t	75.66	52.76	38.22	30.13	26.11	
		tar	160340	150446	141413	140608	140207	
20.0-128.8	SSE _O	3	39	46	21	27	137	
	SSE _S	3	39	38.9	16.0	20.3	117.2	
PT12	t	77.08	53.75	39.80	31.23	26.89		
	tar	160505	150545	141548	140714	140253		
20.0-130.2	SSE _O	5	25	38	20	11	100	
	SSE _S	5	25	35.0	15.8	8.9	89.7	
12 Aug 13	PT4	t	63.96	44.61	31.49	25.00	21.74	
		tar	160358	150836	141929	141300	140945	
22.0-128.2	SSE _O	4	30	31	25	13	105	
	SSE _S	4	30	26.2	19.8	10.5	90.5	
PT12	t	65.28	45.53	32.63	25.74	22.33		
	tar	160517	150932	142038	141345	141020		
22.0-129.6	SSE _O	3	24	20	15	4	67	
	SSE _S	3	24	16.9	11.9	3.2	59	

00 Aug 14	PT4	t	55.00	38.36	26.12	20.80	18.22		
		tar	160700	151422	150207	142048	141819		
	23.5-127.2	S _O	4	17	22	18	17	79	
		S _S	4	17	18.6	13.4	12.4	65.4	
	23.5-128.5	PT12	t	55.85	38.95	27.18	21.63	18.91	
			tar	160751	151457	150311	142138	141855	
SSE _O		4	30	30	28	20	114		
		SSE _S	4	30	25.4	21.3	15.0	95.7	
12 Aug 14	PT4	t	48.68	33.95	22.20	17.59	15.71		
		tar	161241	152157	151012	150535	150343		
	24.6-126.7	S _O	1	19	31	13	8	74	
		S _S	1	19	24.9	9.1	5.4	59.4	
	24.6-128.2	PT12	t	49.34	34.41	23.39	18.73	16.39	
			tar	161320	152224	151123	150614	150424	
SSE _O		1	28	33	34	27	125		
		SSE _S	1	28	27.9	25.9	20.3	103.1	
00 Aug 15	PT4	t	41.32	28.82	18.25	14.27	12.93		
		tar	161719	160449	151815	151416	151256		
	25.9-126.5	S _O	9	40	36	23	22	132	
		S _S	9	40	29.9	17.4	16.0	112.3	
	25.9-128.0	PT12	t	41.89	29.10	19.27	15.53	13.75	
			tar	161753	160513	151916	151532	151345	
SSE _O		3	29	20	17	40	110		
		SSE _S	3	29	16.9	12.9	29.2	91.0	
25.9-128.0	PT12	t	41.89	29.10	19.27	15.53	13.75		
		tar	161753	160513	151916	151532	151345		
	S _O	3	34	41	33	12	125		
		S _S	3	34	34.7	25.4	9.0	106.1	

12 Aug 15	PT4	t	32.36	22.57	11.92	10.21	9.58			
		tar	162022	161034	152355	152213	152135			
	27.5-126.0	S _O	0	19	13	24	15	73		
		S _S	0	19	10.6	17.4	10.5	57.5		
	25.5-125.9	PT8	t	43.73	30.53	18.58	15.16	13.70		
			tar	170744	161832	160635	160310	160142		
		S _O	1	17	15	14	13	62		
			S _S	1	17	12.4	10.4	9.5	50.3	
		27.5-127.5	PT12	t	32.54	22.70	13.78	11.35	10.21	
				tar	162033	161042	160147	152321	152231	
SSE _O	1		21	56	55	75	212			
	SSE _S		1	21	47.4	41	54.8	145.2		
27.5-127.5	PT12	t	32.54	22.70	13.78	11.35	10.21			
		tar	162033	161042	160147	152321	152231			
	S _O	0	17	38	53	43	153			
		S _S	0	17	322	39.9	30.8	119.9		
	00 Aug 16	PT4	t	20.57	14.34	7.41	6.49	6.09		
			tar	162034	161421	160725	160629	160605		
29.6-126.0		S _O	0	15	14	19	15	65		
		S _S	0	15	11.8	15.0	12.2	54		
27.6-126.0		PT8	t	31.79	22.17	11.85	10.03	9.41		
			tar	170747	162210	161151	161002	160925		
		S _O	0	16	20	31	21	90		
			S _S	0	16	16.4	22.5	14.7	69.6	
27.6-126.0		PT8	t	31.79	22.17	11.85	10.03	9.41		
			tar	170747	162210	161151	161002	160925		
	SSW _O	0	33	62	47	31	175			
		SSW _S	0	33	50	32.2	19	134.2		

	PT12	t	20.85	14.54	7.52	6.58	6.17	
		tar	162051	161432	160731	160635	160610	
29.6-127.5		SSE _O	1	24	54	60	38	179
		SSE _S	1	24	45.7	47.5	30.8	149
	PT12	t	20.85	14.54	7.52	6.58	6.17	
		tar	162051	161432	160731	160635	160610	
29.6-127.5		S _O	1	21	40	40	19	122
		S _S	1	21	33.9	29.2	13.3	98.4

c. Typhoon Owen

		\bar{T}	7	10	13	16	19	SUM
06 Sep 25 (GMT)	PT4	t	73.96	51.58	39.39	30.41	26.05	
		tar	280758	270935	262123	261225	260803	
21.3-132.4		SSE _O	7	26	31	8	0	74
		SSE _S	7	26	26.2	6.3	0	65.5
	PT12	t	77.55	54.08	41.62	32.00	27.43	
		tar	281133	271205	262337	261400	260926	
21.1-133.9		SSE _O	5	28	19	14	10	78
		SSE _S	5	28	16.1	11.1	7.8	68
18 Sep 25	PT4	t	65.66	45.79	34.63	26.56	22.89	
		tar	281140	271547	270438	262034	261653	
22.6-131.7		SSE _O	3	38	36	10	0	89
		SSE _S	3	38	30.5	7.3	0	78.8
	PT12	t	68.96	48.09	36.74	28.32	24.32	
		tar	281458	271805	270644	262219	261819	
22.6-133.1		SSE _O	2	27	34	15	9	88
		SSE _S	2	27	28.8	11.9	7.1	76.8

06 Sep 26	PT4	t	60.28	42.04	31.64	24.36	20.07		
		tar	281817	280002	241338	270622	270204		
	22.5-131.4	SSE _O	2	39	54	42	1	140	
		SSE _S	2	39	45.7	32.3	0.7	119.7	
		PT12	t	63.68	44.41	33.76	26.03	22.35	
			tar	282141	280225	271546	270802	270421	
23.5-132.8		SSE _O	2	33	49	26	19	132	
		SSE _S	2	33	41.5	20.6	14.9	112	
18 Sep 26		PT4	t	51.13	35.66	26.55	20.48	17.66	
			tar	282108	280539	272034	271429	271140	
	24.4-131.6	SSE _O	0	32	54	48	53	188	
		SSE _S	0	32	45.7	38	41.5	157.2	
		PT12	t	62.92	43.88	34.5	26.26	22.44	
			tar	290855	281353	280430	272016	271626	
29.4-135.3		SE _O	0	9	15	17	15	57	
		SE _S	0	9	12.7	13.5	12.2	47.4	
06 Sep 27		PT4	t	51.32	35.79	27.92	20.86	17.96	
			tar	290919	281747	280955	280252	272358	
	25.5-131.9	SSE _O	0	17	54	31	56	160	
		SSE _S	0	17	45.7	24.6	45.4	132.7	
		PT12	t	55.75	38.88	30.34	22.67	19.52	
			tar	291345	282053	281220	280440	280131	
25.5-133.4		SE _O	1	9	11	7	8	37	
		SE _S	1	9	93	5.5	6.5	31.3	
18 Sep 27		PT4	t	46.79	32.63	25.24	18.73	16.20	
			tar	291648	290238	281914	281244	281012	
	26.5-132.0	SSE _O	1	30	58	49	39	180	
		SSE _S	1	30	49.1	38.8	31.6	150.5	

	PT4	t	46.79	32.63	25.24	18.73	16.20	
		tar	291648	290238	281914	281244	281012	
	26.5-132.0	SE _O	0	26	57	81	35	201
		SE _S	0	26	48.2	64.2	28.4	166.8
	PT6	t	38.30	26.71	19.76	14.94	13.01	
		tar	290818	282043	281346	280857	280706	
	28.5-132.1	SE _O	1	18	39	32	30	123
		SE _S	1	18	33	25.3	24.3	101.6
	PT12	t	51.60	35.99	28.08	21.03	18.04	
		tar	292136	290559	280205	281502	281202	
	26.5-133.5	SE _O	0	15	18	23	17	75
		SE _S	0	15	15.2	18.2	13.8	62.2
06 Sep 28	PT4	t	43.40	30.26	23.43	17.31	14.99	
		tar	300124	291216	290526	282319	282059	
	27.3-132.1	SE _O	1	26	44	52	36	161
		SE _S	1	26	37.2	41.2	29.2	134.6
	PT12	t	48.21	33.62	25.44	19.61	16.86	
		tar	300612	291537	290726	290136	282252	
	27.3-133.5	SE _O	1	15	25	24	14	81
		SE _S	1	15	21.2	19	11.3	67.5
18 Sep 28	PT4	t	41.13	28.68	22.05	16.29	14.14	
		tar	301108	292241	291603	291017	290608	
	27.8-132.1	SE _O	1	10	15	16	5	49
		SE _S	1	10	12.7	12.7	4.0	40.4
06 Sep 29	PT4	t	39.25	27.37	21.18	15.70	13.58	
		tar	302115	300922	300311	292142	291935	
	28.5-132.4	SE _O	2	10	18	12	11	55
		SE _S	2	10	15.2	9.5	8.9	45.6

LIST OF REFERENCES

1. Pierson, W. J., G. Neumann, and R. W. James, 1955, Practical Methods for Observing and Forecasting Ocean Waves by Means of Wave Spectra and Statistics, Naval Oceanographic Office, H. O. Pub. 603, 284 pp.
2. Murray, T. R., and D. R. Morford, 1979, 1979 Annual Typhoon Report, Joint Typhoon Warning Center, Guam, Marina Islands, 191 pp.
3. Kauffmann, C. F., 1973, Swell Prediction by A Multiple Point-Source Swell Generation Model, Master's Thesis, Naval Postgraduate School, Monterey, 73 pp.
4. Czaja, B. F., and D. W. Stevenson, 1964, Simplified Spectral Forecasts of Sea and Swell Waves by Graphical Means, Master's Thesis, Naval Postgraduate School, Monterey, 307 pp.
5. U.S. Army, Corps of Engineers, 1977, Shore Protection Manual Volume I, U. S. Army Coastal Engineering Research Center, 4-180 pp.
6. U.S. Army, Corps of Engineers, 1977, Shore Protection Manual Volume III, U.S. Army Coastal Engineering Research Center, D-15 pp.
7. U.S. Army, Corps of Engineers, 1953, Analysis of Moving Fetches for Wave Forecasting, Technical Memorandum No. 35, 39 pp.
8. U.S. Navy Hydrographic Office, 1951, Techniques for Forecasting Wind Waves and Swell, H.O. Pub. No. 604, U.S. Navy Hydrographic Office, Washington, DC, 37 pp.
9. U.S. Army, Corps of Engineers, 1953, On Ocean Wave Spectra and A New Method of Forecasting Wind-Generated Sea, Technical Memorandum No. 43, Beach Erosion Board, Office of the Chief of Engineers, Washington, DC, 42 pp.
10. U.S. Army, Corps of Engineers, 1955, Graphical Approach to the Forecasting of Waves in Moving Fetches, Technical Memorandum No. 73, Beach Erosion Board, Office of the Chief of Engineers, Washington, DC, 31 pp.

11. Brand, S., K. Rake, and T. Laevastu, 1977, Parameterization Characteristics of a Wind-Wave Tropical Cyclone Model for the Western North Pacific Ocean, Journal of Physical Oceanography, Vol. 7, No. 5, September 1977, pp. 739-746.
12. Brand, S., J. W. Blelloch, and D. C. Schertz, 1974, State of the Sea Around Tropical Cyclones in the Western North Pacific Ocean, Journal of Applied Meteorology, Vol. 14, No. 1, February 1975, pp. 25-30.
13. Brand, S., Rabe, K., and T. Laevastu, 1976, A Wind Wave Tropical Cyclone Model for the Western North Pacific Ocean, NAVENVPREDRSCHFAC Technical Paper No. 8-76, Naval Environmental Prediction Research Facility, Monterey, CA 93940.
14. Reynolds, F. M., 1976, Climatological Wave Statistics Derived from FNWC Synoptic Spectral Wave Analyses, Master's Thesis, Naval Postgraduate School, Monterey, CA 93940, 141 pp.
15. Sediny, D. G., 1978, Ocean Wave Group Analysis, Master's Thesis, Naval Postgraduate School, Monterey, CA 93940, 90 pp.
16. Hubert, W. E. and B. R. Mendenhall, 1970, The FNWC Singular Sea/Swell Model, Fleet Numerical Weather Central, Monterey, CA 93940.
17. Brand, S., et al, 1978, An Analysis of Western North Pacific Tropical Cyclone Forecast Errors, Monthly Weather Review, Vol. 106, No. 7, July 1978, pp. 925-937.
18. Verploegh, G., 1961, On the Accuracy and the Interpretation of Wave Observations from Selected Ships, WMO Commission for Maritime Meteorology working Paper.

INITIAL DISTRIBUTION LIST

	No. Copies
1. Defense Technical Information Center Cameron Station Alexandria, Virginia 22314	2
2. Library, Code 0142 Naval Postgraduate School Monterey, California 93940	2
3. Chairman, Code 68 Department of Oceanography Naval Postgraduate School Monterey, California 93940	1
4. Chairman, Code 63 Department of Meteorology Naval Postgraduate School Monterey, California 93940	1
5. Professor J. B. Wickham, Code 68Wk Department of Oceanography Naval Postgraduate School Monterey, California 93940	1
6. LCDR Lee, Hyong Sun Korean Naval Academy Jin Hae, Kyung Nam, KOREA	2
7. Academic Dean Korean Naval Academy Jin Hae, Kyung Nam, KOREA	1
8. ADCNO for Education and Training Division Korea Navy HQs Seoul, KOREA	1
9. Dr. Na, Jung Yul Jin Hae Machine Depot P.O. Box 18 Jin Hae, Kyung Nam, KOREA	1
10. Chairman, Department of Oceanography Seoul National University Kwanak-Gu Seoul, KOREA	1

- | | | |
|-----|---|---|
| 11. | Chairman, Department of Meteorology
Seoul National University
Kwanak-Gu, Seoul, KOREA | 1 |
| 12. | Dr. Lee, Byung Don
Director
Korea Research Institute of Ocean
P.O. Box 151
39-1 Hawolgok-dong
Sungbuk-Gu, Seoul, KOREA | 1 |
| 13. | Commanding Officer
Fleet Numerical Oceanography Center
Monterey, California 93940 | 1 |
| 14. | Director, Naval Oceanography Division
Navy Observatory
34th and Massachusetts Avenue NW
Washington, DC 20390 | 1 |
| 15. | Commander
Naval Oceanography Command
NSTL Station
Bay St Louis, Mississippi 39529 | 1 |
| 16. | Commanding Officer
Naval Environmental Prediction Research
Facility
Monterey, California 93940 | 1 |
| 17. | Samson Brand
Naval Environmental Prediction Research
Facility
Monterey, California 93940 | 1 |
| 18. | Library
Scripps Institution of Oceanography
P.O. Box 2367
La Jolla, California 92037 | 1 |
| 19. | Library
School of Oceanography
Oregon State University
Corvallis, Oregon 97331 | 1 |
| 20. | Chairman
Oceanography Department
U.S. Naval Academy
Annapolis, Maryland 21402 | 1 |

DATE
ILME